Biochimica et Biophysica Acta xxx (2016) xxx–xxx

Contents lists available at ScienceDirect

Biochimica et Biophysica Acta

journal homepage: www.elsevier.com/locate/bbagen

Glycosylation-dependent binding of galectin-8 to activated leukocyte cell adhesion molecule (ALCAM/CD166) promotes its surface segregation on breast cancer cells

Marisa M. Fernández [a,1], Fátima Ferragut [b,1], Víctor M. Cárdenas Delgado [b], Candelaria Bracalente [b], Alicia I. Bravo [c], Alejandro J. Cagnoni [d], Myriam Nuñez [e], Luciano G. Morosi [d,f], Héctor R. Quinta [b], María V. Espelt [b], María F. Troncoso [b], Carlota Wolfenstein-Todel [b], Karina V. Mariño [d], Emilio L. Malchiodi [a], Gabriel A. Rabinovich [f,g], María T. Elola [b,*]

[a] Institute of Studies in Humoral Immunology, University of Buenos Aires (UBA) and National Council Research (CONICET), Microbiology, Immunology and Biotechnology Department, School of Pharmacy and Biochemistry, University of Buenos Aires (UBA), Buenos Aires, Argentina
[b] Institute of Biochemistry and Biophysics (IQUIFIB), UBA-CONICET, Biological Chemistry Department, School of Pharmacy and Biochemistry, UBA, Buenos Aires, Argentina
[c] Molecular Pathology Department, "Eva Perón" HIGA Hospital, Buenos Aires, Argentina
[d] Laboratory of Functional and Molecular Glycomics, Institute of Biology and Experimental Medicine (IBYME), CONICET, Buenos Aires, Argentina
[e] Department of Mathematics and Statistics, School of Pharmacy and Biochemistry, UBA, Buenos Aires, Argentina
[f] Laboratory of Immunopathology, IBYME, CONICET, Buenos Aires, Argentina
[g] Faculty of Exact and Natural Sciences, UBA, Buenos Aires, Argentina

ARTICLE INFO

Article history:
Received 9 December 2015
Received in revised form 27 March 2016
Accepted 23 April 2016
Available online xxxx

Keywords:
ALCAM/CD166
Breast cancer cell
Galectin-8
Physical interaction
Receptor segregation

ABSTRACT

Background: We previously demonstrated that the *activated leukocyte cell adhesion molecule* (ALCAM/CD166) can interact with galectin-8 (Gal-8) in endothelial cells. ALCAM is a member of the immunoglobulin superfamily that promotes homophilic and heterophilic cell–cell interactions. Gal-8 is a "*tandem-repeat*"-type galectin, known as a matricellular protein involved in cell adhesion. Here, we analyzed the physical interaction between both molecules in breast cancer cells and the functional relevance of this phenomenon.
Methods: We performed binding assays by surface plasmon resonance to study the interaction between Gal-8 and the recombinant glycosylated ALCAM ectodomain or endogenous ALCAM from MDA-MB-231 breast cancer cells. We also analyzed the binding of ALCAM-silenced or control breast cancer cells to immobilized Gal-8 by SPR. In internalization assays, we evaluated the influence of Gal-8 on ALCAM surface localization.
Results: We showed that recombinant glycosylated ALCAM and endogenous ALCAM from breast carcinoma cells physically interacted with Gal-8 in a glycosylation-dependent fashion displaying a differential behavior compared to non-glycosylated ALCAM. Moreover, ALCAM-silenced breast cancer cells exhibited reduced binding to Gal-8 relative to control cells. Importantly, exogenously added Gal-8 provoked ALCAM segregation, probably trapping this adhesion molecule at the surface of breast cancer cells.
Conclusions: Our data indicate that Gal-8 interacts with ALCAM at the surface of breast cancer cells through glycosylation-dependent mechanisms.
General significance: A novel heterophilic interaction between ALCAM and Gal-8 is demonstrated here, suggesting its physiologic relevance in the biology of breast cancer cells.

Abbreviations: 2AB, 2-aminobenzamide; ALCAM, Activated leukocyte cell adhesion molecule; ALCAMe, Endogenous ALCAM from MDA-MB-231 cells; ALCAMgly, Recombinant glycosylated ALCAM expressed in HEK-293 cells; ALCAMnongly, Non-glycosylated ALCAM; ADAM17, A disintegrin and metalloprotease 17; CM, Conditioned medium; CRD, Carbohydrate recognition domain; DABCO, Diazabicyclo[2.2.2]octane; DCIS, Ductal carcinoma *in situ*; EDTA, Ethylene-diaminetetraacetic acid; EEA1, Early endosomal antigen 1; ER, Estrogen receptor; FBS, Fetal bovine serum; FITC, Fluorescein isothiocyanate; FV, Coagulation factor V; Gal-8, Galectin-8; Gal-1, Galectin-1; Gal-3, Galectin-3; GAPDH, Glyceraldehyde 3-phosphate dehydrogenase; HER2 = Her2-neu, Human epidermal growth factor receptor 2; HRP, Horseradish-peroxidase; IDC, Invasive ductal carcinoma; IL-2, Interleukin 2; k*on*, Association rate; k*off*, Dissociation rate; Lys, Cell lysates; PBS, Phosphate-buffered saline; PerCP-Cy5.5, Peridinin-chlorophyll protein (PerCP)-cyanine (Cy) 5.5; PMSF, Phenylmethylsulfonyl fluoride; PVDF, Polyvinylidene-difluoride; rGal-8, Recombinant galectin-8; RU, Resonance unit; SDS-PAGE, Sodium dodecyl sulphate–polyacrylamide gel electrophoresis; shALCAM, shRNA specific for ALCAM; SPR, Surface plasmon resonance; TDG, Thiodigalactoside; TGF-β, Transforming growth factor-beta; WAX, Weak Anionic Exchange chromatography.

* Corresponding author at: Institute of Biochemistry and Biophysics (IQUIFIB), UBA-CONICET, Biological Chemistry Department, School of Pharmacy and Biochemistry, University of Buenos Aires, Junín 956, C1113AAD, Buenos Aires, Argentina.
E-mail address: mt_elola@yahoo.com (M.T. Elola).
[1] These authors contributed equally to this work.

http://dx.doi.org/10.1016/j.bbagen.2016.04.019
0304-4165/

1. Introduction

The activated leukocyte cell adhesion molecule (ALCAM) or CD166 is a member of the immunoglobulin superfamily with five extracellular immunoglobulin-like domains, which functions as a cell–cell adhesion molecule in homophilic (ALCAM-ALCAM) and heterophilic (ALCAM-CD6) interactions between adjacent cells in different tissues [1,2]. Cancer-associated ALCAM was first identified in melanoma cell lines [3], and it was subsequently found in different cell lines including breast, lung, colon, and prostate [4]. ALCAM has been proposed as a biomarker of cancer progression in prostate cancer [5,6], breast cancer [7–9], colorectal cancer [10], oral cancer [11,12], pancreatic cancer [13], neuroblastoma [14], ovarian cancer [15], and melanoma [16]. Cell–cell adhesion is the primary known function of ALCAM, being regulated by ALCAM availability to bind to proximal partners at the cell surface. For example, immunohistochemical staining of prostate cancer tissue microarrays revealed that ALCAM was clearly evident in both normal, low-, and medium-grade disease but was reduced at the tumor cell surface in high-grade disease [5], as suggested [11,13,15,17,18]. In fact, ALCAM expression at the cell surface can be modulated by ligand-induced internalization and recycling [19,20], and by proteolytic cleavage of its ectodomain (shedding) mediated by ADAM17 (a disintegrin and metalloprotease) [5,21,22]. Importantly, we have shown for the first time that ALCAM serves as a receptor for the endogenous lectin galectin-8 (Gal-8) in endothelial cells [23]. Galectin-8 (Gal-8) is a bivalent "*tandem-repeat*"-type galectin, which possesses two carbohydrate recognition domains (CRDs) with β-galactoside affinity that are connected by a linker peptide. Gal-8 shows a complex gene regulation, giving rise to numerous messenger RNAs, and at least seven isoforms [24,25]. The specificity and affinity of Gal-8 for saccharide ligands was previously described, showing a preference for α(2,3)-sialylated glycans and 3-sulfated glycans [26,27]. Ideo and coworkers reported a K_D of 2.7 μM for α(2,3) sialyllactose, and K_D of 1.9 μM for 3′-sulfated lactose (SO3-3′Lac) [27]. Adhesion of CHO cells and affinity experiments suggested that Gal-8 binds to glycoproteins on the cell surface [26]. Several Gal-8 receptors have been described in different cells and tissues, including integrins [28–30], pro-metalloproteinase-9 [31], CD44vRA [32], coagulation factor V (FV) [33], podoplanin [34], and nuclear dot protein 52 kDa (NDP52) [35]. This lectin has been described as a modulator of different cell functions including cell adhesion, spreading [28–30], growth arrest and apoptosis [36], pathogen recognition [37], autophagy [35], and generation of regulatory T cells [38]. Gal-8 is one of the most widely expressed bi-CRD galectins in human tissues, being detected in normal and tumor cells [39–41].

Here we aimed to analyze the physical interaction between ALCAM and Gal-8 in human breast cancer cells to bring insights on the *in vivo* potential relationship between both molecules. Surface plasmon resonance (SPR) experiments revealed that Gal-8 physically interacts with recombinant glycosylated ALCAM ectodomain and endogenous ALCAM from breast cancer cells in a glycan-dependent manner. Moreover, ALCAM-silenced breast cancer cells showed reduced binding to immobilized Gal-8 relative to control cells, which bound to Gal-8-coated substrates in a glycan-dependent fashion. Importantly, extracellular Gal-8 provoked receptor segregation, probably trapping ALCAM at the surface of breast cancer cells. Altogether, our results suggest that the Gal-8/ALCAM axis is active at the surface of breast cells and might influence cell–cell and cell–matrix interactions in healthy tissues and during tumor progression.

2. Materials and methods

2.1. Cell culture

MDA-MB-231 (ATCC HTB-26), MCF-7 (ATCC HTB-22), and T47D (ATCC HTB-133) human breast cancer, and HEK-293 (ATCC CRL-1573) human embryonic kidney cell lines were obtained from ATCC (Rockville, MD, USA). Breast cancer cells were cultured in Dulbecco's modified Eagle's medium containing 4.5 g/l glucose, supplemented with 10% heat-inactivated fetal bovine serum (FBS, Natocor, Villa Carlos Paz, Argentina), 2 mM L-glutamine, 100 μg/ml streptomycin, and 100 units/ml penicillin. HEK-293 cells were cultured in Eagle's minimum essential medium supplemented with 10% FBS, 2 mM L-glutamine, 100 μg/ml streptomycin, and 100 units/ml penicillin. For analysis of Gal-8 secretion, subconfluent cell monolayers were cultured with or without FBS for 24–48 h, and then conditioned media were collected and centrifuged for 10 min at 400 × *g*; sodium dodecyl sulfate (SDS) was added to the supernatants to a 0.5% (w/v) final concentration, then heated at 100 °C for 10 min, and diluted with 1:10 methanol, followed by an overnight incubation at −20 °C; after centrifugation at 21,000 × g for 30 min, pellets were recovered and protein concentration was determined.

2.2. Indirect immunofluorescence

Immunofluorescence was performed to detect ALCAM and Gal-8 in MDA-MB-231, MCF-7, and T47D cells. Cells were grown on uncoated coverslips in 24-well plates for 48 h. Cells were then rinsed twice in cold PBS and fixed in 4% paraformaldehyde at 0 °C for 30 min. After washing, cells were blocked and permeabilized in 5% heat-inactivated human serum plus 0.05% saponin in PBS for 1 h. Some coverslips were stained for Gal-8, incubating with a polyclonal anti-Gal-8 antibody (1:50; AF1305; R&D Systems, Minneapolis, MN, USA); after washing, samples were incubated with Alexa Fluor 488-conjugated secondary antibody (1:1,000; A11055; Molecular Probes, Invitrogen, Carlsbad, CA, USA) for 1 h. Staining for ALCAM was performed on other coverslips by incubating with an anti-ALCAM monoclonal antibody (1:40; NCL-CD166, clone MOG/07; Novocastra–Leica, Newcastle, UK), followed by Alexa Fluor 555-conjugated secondary antibody (1:1,000; 4409; Cell Signaling, Danvers, MA, USA) for 1 h. Negative controls were performed by substituting the primary antibody by PBS, followed by the corresponding secondary antibody. Samples were mounted in diazabicyclo[2.2.2]octane (DABCO; Fluka, Steinheim, Germany) and observed under a Fluo View FV1000 confocal microscope (Olympus, Tokyo, Japan).

2.3. Endogenous ALCAM isolation

The anti-ALCAM monoclonal antibody (Novocastra–Leica) was coupled to MabSelect SuRe LX alkali-tolerant protein A, a matrix with high binding capacity for monoclonal antibodies (GE Healthcare, Piscataway, NJ, USA). Coupling to the matrix was performed in 25 mM Tris–HCl, pH 7.8, for 2 h at 4 °C, under the manufacturer's instructions. Clarified whole lysates from MDA-MB-231 breast cancer cells in 25 mM Tris–HCl, pH 7.8, were loaded onto beads and incubated for 3 h on ice. ALCAM elution from the antibody was performed in 25 mM Tris–HCl, pH 10.0, and pH was immediately neutralized with 5 N HCl. Alternatively, for isolation of endogenous ALCAM, we performed affinity chromatography in a Gal-8-Affi-Gel 10 column, which was prepared as previously described [23], loaded with MDA-MB-231 cell supernatants and eluted with 100 mM lactose. Eluted fractions were analyzed by Western blot and mass spectrometry [23] to detect ALCAM.

2.4. shRNA-mediated ALCAM knockdown

To establish a MDA-MB-231 cell line in which ALCAM/CD166 expression was stably knocked-down, cells were transduced with ALCAM-specific shRNA lentiviral particles (sc-43023-V, Santa Cruz Biotech., CA, USA), following the manufacturer's instructions. Control lentivirus (sc-108080), carrying scrambled-shRNA, was used for mock transduction. Finally, cells were selected in 1 μg/ml puromycin, ALCAM expression was evaluated by Western blot, and ALCAM knocked-down or mock-transduced cells were cultured and maintained in 1 μg/ml puromycin-containing culture medium.

Please cite this article as: M.M. Fernández, et al., Glycosylation-dependent binding of galectin-8 to activated leukocyte cell adhesion molecule (ALCAM/CD166) promotes its surface seg..., Biochim. Biophys. Acta (2016), http://dx.doi.org/10.1016/j.bbagen.2016.04.019

2.5. Surface plasmon resonance (SPR)

The interaction of recombinant glycosylated and endogenous ALCAM with Gal-8 was measured by SPR analysis using a BIAcore T100 instrument (GE, Piscataway, NJ, USA). Briefly, recombinant human ALCAM ectodomain (expressed in HEK-293 embryonic kidney cells; Sino Biological, Beijing, China) was resuspended in sodium acetate, pH 5.0, and coupled to the carboxymethyl-dextran matrix of CM5 sensor chips (BIAcore) using the Amine Coupling kit. Recombinant human non-glycosylated ALCAM (Abnova Corporation, Taipei, Taiwan) was also coupled to CM5 chips for comparison. Recombinant Gal-8 and galectin-1 (Gal-1) were purified as previously described [23,42]. Micromolar concentrations (0–10 μM) of the plant lectin concanavalin A (Con A; Sigma–Aldrich, St. Louis, MO, USA), recombinant Gal-8 and Gal-1 were tested in two-fold dilutions for specific binding. Interactions between Gal-8 and ALCAM were also determined in the presence of 20 mM sucrose and lactose or 1 mM thiodigalactoside (TDG). SPR data were analyzed using BIAEvaluation software [43]. In cell binding assays, 500,000 cells/ml in PBS were loaded onto Gal-8 (400 resonance units, RU) coupled to CM5 BIAcore chips.

2.6. N-Glycan profiling

2.6.1. N-Glycan release and 2-aminobenzamide-labeling

N-glycans were released from ALCAMgly using a previously described method [44]. Briefly, protein was reduced and alkylated in solution. Then, the *N*-linked glycans were released using peptide *N*-glycanase F (1000 U/mL; Roche, Manheim, Germany) for 16 h, at 37 °C and the digested glycans were separated by filtration (Nanosep 10K Omega, Pall Life Sciences, New York, NY, USA). Glycans were subsequently fluorescently labeled with 2-aminobenzamide (2AB) by reductive amination [44] and excess of 2AB was removed by paper chromatography [44] or by LudgerClean S Cartridges (Ludger Ltd., Oxford, UK). ALCAMe was purified by affinity chromatography [23], blotted onto polyvinylidene-difluoride (PVDF) membranes (Bio Rad, Hercules, CA, USA), and then detected by immunoblotting (Section 2.8). *N*-glycans were released from the membrane as previously described [45]. Released *N*-glycans were then labeled as described for ALCAMgly.

2.6.2. Weak Anionic Exchange Chromatography with fluorescence detection (WAX-FLR)

Separation of neutral and acidic oligosaccharides by Weak Anion Exchange (WAX) chromatography (WAX-HPLC) was performed using a BioSuite DEAE 2.5 μm NP AXC 4.6 × 35 mm column (Waters, Milford, MA, USA) on an Acquity H-class UPLC system (Waters) equipped with a temperature control module (Waters). Solvent A was ammonium acetate 50 mM (pH 7.0) in 20% v/v acetonitrile, and solvent B was 20% aqueous acetonitrile. Gradient conditions were as follows: an initial equilibration of 2 min of 0% A, a linear gradient of 0–40% A over 4 min at a flow rate of 0.5 mL/min, followed by 40–100% A over 3 min, then 4 min at 100% A, 100 to 0% A over 0.5 min, and then 3.5 min at 0% A. Samples were injected in water and fetuin *N*-glycans were used for calibration [46].

2.6.3. Neuraminidase digestion profiling for sialylation analysis

As both sialic acid and sulfate addition to glycans provide negative charge to 2AB-labeled structures, sulfated structures were eliminated by digestion with α(2–3, 6, 8, 9) Neuraminidase A (cloned from *Arthrobacter ureafaciens*, 50 U/assay, New England Biolabs, Ipswich, MA, USA). Percentage of α(2,3) sialic acid was determined by the specific action of an α(2,3) Neuraminidase (cloned from *Salmonella typhymurium*, 500 U/assay, New England Biolabs). Enzymatic digestions were performed on 2AB-labeled *N*-glycans in manufacturer's recommended buffers for 16 h at 37 °C. After digestion, *N*-glycans were separated from sialidases before chromatographic analysis by centrifugation in a Nanosep 10K Omega microcentrifuge filter (Pall Life Sciences).

2.7. Real-time quantitative RT-PCR

RNA was purified using TRIzol reagent (Life Technologies, Thermo Fisher Scientific, Waltham, MA, USA) and DNAse (Promega, Madison, WI, USA). cDNA was synthetized using M-MLV reverse transcriptase (Promega), according to the manufacturer's instructions in the presence of random hexamers (2.5 μg/mL) and deoxynucleotide triphosphates (dNTP; 500 nmol/L). Relative gene expression was analyzed using SYBR Green PCR Master Mix (Applied Biosystem, Thermo Fisher Scientific) and ABI PRISM 7500 Sequence Detection Software (Applied Biosystem). Primers used were human ALCAM forward 5′-AGTGCTACATCCCCTTGA-3′ and reverse 5′-GTGGAAGTCATGGTATAG-3′; human GAPDH forward 5′-CCCACTCCTCCACCTTTGAC-3′ and reverse 5′-CATACCAGGAAATGAG CTTGACAA-3′.

2.8. Western blot analysis

Cells were homogenized in lysis buffer (100 mM Tris, pH 7.4, 1% v/v Triton X-100, 10 mM EDTA, 100 mM sodium pyrophosphate, 4 mM PMSF). Cell lysates were centrifuged for 10 min at 12,000 × *g* at 4 °C, supernatants were collected and protein concentration was determined. Samples from cell lysates or conditioned media (30 μg of protein/lane) were separated by 10% SDS-PAGE, and then electrotransferred onto PVDF membranes. Blots were probed with the anti-ALCAM monoclonal antibody (Novocastra–Leica) or the polyclonal anti-Gal-8 antibody overnight at 4 °C. Detection of β-actin with anti-β-actin antibody (Sigma–Aldrich) was used to normalize protein loading in cell lysates. After incubating with the corresponding horseradish-peroxidase (HRP)-conjugated secondary antibodies, immunoreactive bands were detected by chemiluminiscence (Pierce ECL Plus Western Blotting Substrate, Thermo Fisher Scientific). Densitometric analysis of protein levels was performed using *ImageJ* software (U.S. National Institutes of Health, Bethesda, MD, USA; http://rbsweb.nih.gov/ij/).

2.9. Flow cytometry analysis

For flow cytometry, non-permeabilized human breast cancer cells were blocked in 5% heat-inactivated human serum and incubated with a monoclonal antibody anti-ALCAM conjugated to PerCP-Cy5.5 (1:40; 562131, clone 3A6; Becton Dickinson Pharmingen, San Diego, CA, USA) or an isotype-matched control antibody for 2 h on ice. After washing, cells were fixed in 4% paraformaldehyde. Stained cells were analyzed by flow cytometry in a PASS III flow cytometer (Partec, Görlitz, Germany). Twenty thousand events were acquired for each sample and data analysis was performed by using the WinMDI software program.

2.10. Gal-8 cell surface binding and internalization assays

Recombinant Gal-8 was expressed and purified as previously described [23]. MDA-MB-231 cells grown on uncoated coverslips in 24-well plates were rinsed twice in cold PBS. For galectin surface labeling, non-permeabilized cells were incubated with 1 μM recombinant Gal-8 or PBS at 0 °C for 30 min. After washing in ice-cold PBS, cells were fixed in 4% paraformaldehyde at 0 °C for 60 min. Slides were first incubated with the anti-Gal-8 antibody overnight at 4 °C; after washing, samples were incubated with Alexa Fluor 488-conjugated secondary antibody (1:1,000; A11055; Molecular Probes, Invitrogen, Carlsbad, CA, USA). Staining for ALCAM was performed by incubating with anti-ALCAM (1:40; Novocastra), followed by Alexa Fluor 555-conjugated secondary antibody (1:1000; 4409; Cell Signaling, Danvers, MA, USA). Samples were mounted in DABCO and observed under a Fluo View FV1000 confocal microscope. Antibody-based internalization assays were performed by pre-incubating MDA-MB-231 cells grown on coverslips in the presence of recombinant Gal-8 (4–8 μM), Gal-1 (4–8 μM) or PBS at 0 °C for 30 min. After washing, anti-ALCAM-PerCP-Cy5.5 monoclonal antibody was added and incubated at 0 °C for 2 h. Then,

Please cite this article as: M.M. Fernández, et al., Glycosylation-dependent binding of galectin-8 to activated leukocyte cell adhesion molecule (ALCAM/CD166) promotes its surface seg..., Biochim. Biophys. Acta (2016), http://dx.doi.org/10.1016/j.bbagen.2016.04.019

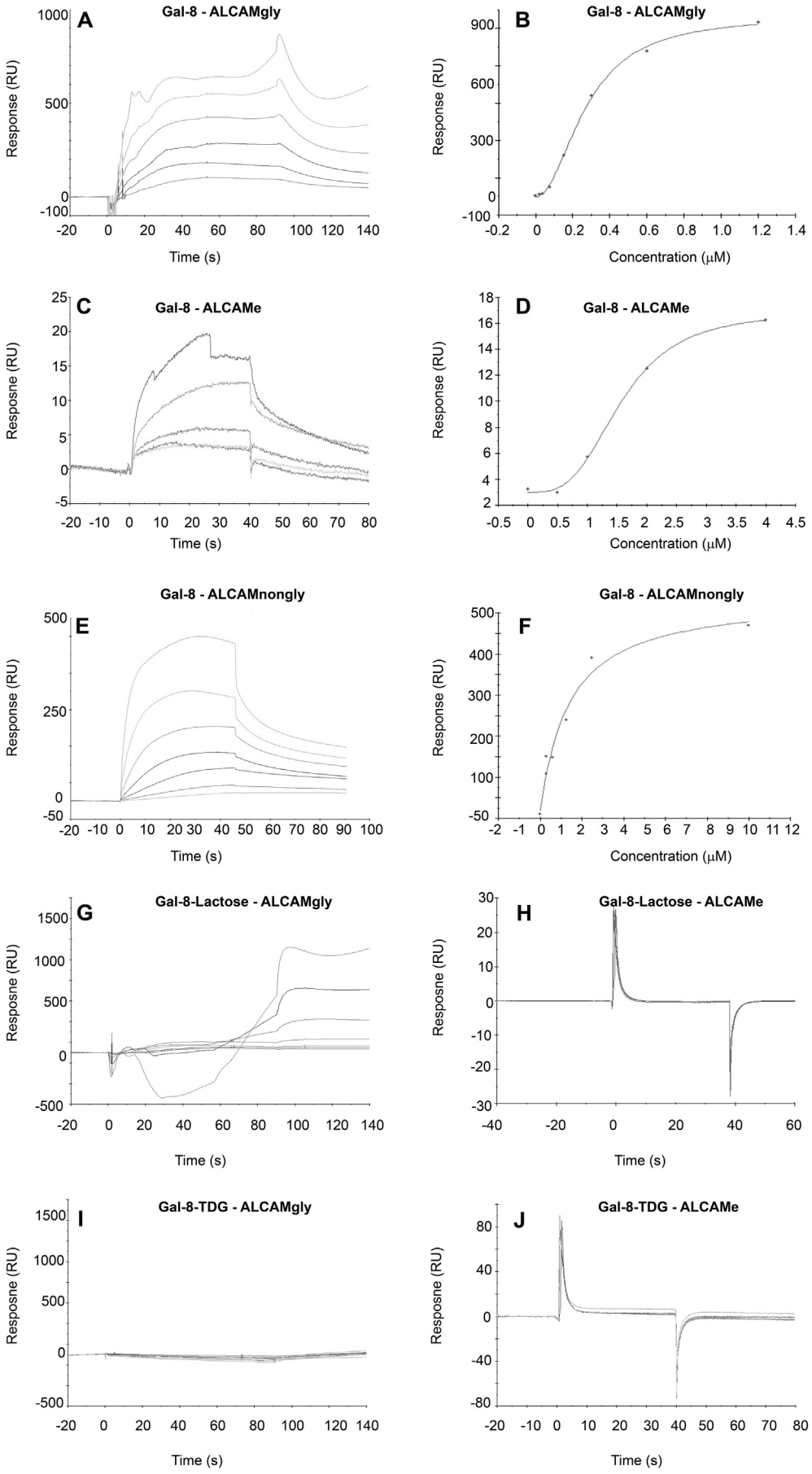

Please cite this article as: M.M. Fernández, et al., Glycosylation-dependent binding of galectin-8 to activated leukocyte cell adhesion molecule (ALCAM/CD166) promotes its surface seg..., Biochim. Biophys. Acta (2016), http://dx.doi.org/10.1016/j.bbagen.2016.04.019

Table 1
Parameters of the interaction between ALCAM and Gal-8: kinetic analysis by surface plasmon resonance.

	K_D (M)	*Kon* ($M^{-1}s^{-1}$)	*koff* (s^{-1})
Human ALCAM:			
Commercial recombinant non-glycosylated ectodomain*	2.10×10^{-6}	$(3.29 \pm 0.43) \times 10^{3}$	$(7.05 \pm 0.09) \times 10^{-3}$
Commercial recombinant glycosylated ectodomain	1.09×10^{-7}	$(2.32 \pm 0.01) \times 10^{4}$	$(2.55 \pm 0.08) \times 10^{-3}$
Endogenous**	3.19×10^{-6}	$(1.58 \pm 0.06) \times 10^{4}$	$(5.04 \pm 0.70) \times 10^{-2}$

* Taken from [23].
** Isolated from MDA-MB-231 breast cancer cells.

internalization was conducted at 37 °C for 0–60 min. After washing, cells were fixed in 4% paraformaldehyde, blocked and permeabilized in 0.05% saponin-5% heat-inactivated human serum-PBS. Finally, cells were incubated with a polyclonal anti-EEA1 antibody (1:100; E-3906; Sigma–Aldrich) and the corresponding fluorescein isothiocyanate (FITC)-conjugated secondary antibody (1:50; Becton Dickinson). In some experiments, 20 mM lactose (Sigma–Aldrich) was added in the culture medium at 37 °C for 48 h, before incubating with Gal-8. For Gal-8 immunofluorescence staining after internalization at 37 °C for 30 min, cells were fixed, blocked, and incubated with the anti-Gal-8 antibody overnight at 4 °C. After washing, samples were incubated with Alexa Fluor 488-conjugated secondary antibody. Samples were mounted in DABCO and observed under a Fluo View FV1000 confocal microscope.

2.11. Immunohistochemistry

Archival paraffin-embedded breast tissue samples were obtained from Molecular Pathology Department, "Eva Perón" HIGA Hospital. The corresponding primary tumor biopsies were obtained from an untreated cohort of patients submitted to surgery at diagnosis, who signed the corresponding informed consents. Ethical approval was obtained according to the rules of the Ethics Committee of "Eva Perón" HIGA Hospital (Buenos Aires, Argentina), in accordance with procedures formulated in the Code of Ethics of the World Medical Association (Declaration of Helsinki). Breast tissue samples corresponding to 10 ductal carcinomas *in situ* (DCIS), 10 invasive ductal carcinomas (IDC), and 10 adjacent normal tissues from mastectomies were analyzed. Diagnoses were made by two pathologists after microscopic review of hematoxylin and eosin-stained slides. Sections obtained from paraffin-embedded specimens were de-paraffinized and rehydrated. Endogenous peroxidase was quenched with 9% H_2O_2 in 100% ethanol. Antigen retrieval was performed by immersing the sections in 10 mM sodium citrate buffer, pH 6.0, at 98 °C for 30 min in a water bath. After blocking, sections were incubated overnight at 4 °C with the polyclonal anti-Gal-8 antibody (10 μg/ml), which does not cross-react with other galectin family members. Other sections were stained with the anti-ALCAM monoclonal antibody (1:40; Novocastra–Leica), and incubated overnight at 4 °C. After washing, the corresponding biotinylated secondary antibodies (1:200; Vector) were added and incubated for 30 min. Immunoreactions were amplified using the avidin–biotin–peroxidase complex method (Vectastain ABC, Vector), followed by 3,3′-diamino-benzidine/H_2O_2 as chromogenic substrate (Vector) according to the manufacturer's instructions. Samples were counterstained with hematoxylin, dehydrated, and mounted. Sections were treated in parallel without primary antibody to provide negative controls. The immunostained samples were viewed and quantified by two observers independently in a blinded manner. Five views were examined per slide, and around 100 cells were observed per view. Cell staining intensity was graded as absent (0), weak (1+), moderate (2+), or strong (3+).

2.12. Statistical analysis

Data were analyzed using GraphPad Prism Software (GraphPad Software Inc., La Jolla, CA, USA) and results are expressed as the mean ± SD from, at least, three independent experiments. Differences between groups were assessed by Student's *t*-test or one-factor ANOVA with appropriate post-tests. Values of $p < 0.05$ are considered statistically significant.

3. Results

3.1. ALCAM and Gal-8 physically interact in BIAcore chips

We have recently established that ALCAM is a Gal-8-binding partner in endothelial cells [23]. We undertook this study to analyze the Gal-8/ALCAM axis in breast cancer cells. We first studied the interaction between human recombinant glycosylated ALCAM (ALCAMgly), expressed in HEK-293 human cells, and Gal-8 by SPR (Fig. 1A, Table 1). The apparent K_D for Gal-8 binding to immobilized ALCAMgly was 2.51×10^{-7} M by steady state affinity analysis and 1.09×10^{-7} M by kinetic analysis, suggesting a specific interaction between these two molecules and no significant differences between the two methods employed. Next, we compared the interaction of Gal-8 with both recombinant ALCAMgly and endogenous ALCAM (ALCAMe). To identify cells with higher amounts of endogenous ALCAM, we analyzed ALCAM expression levels in different breast cancer cells by immunofluorescence using confocal microscopy (Fig. 3A). ALCAM was strongly expressed in the cytoplasm of permeabilized MDA-MB-231 cells and to a lesser extent in permeabilized MCF-7 cells, but it was almost absent in T47D cells (Fig. 3A). Gal-8 was detected in the cytoplasm and in some nuclei of MDA-MB-231 and MCF-7 permeabilized cells, but was faintly observed in T47D cells under similar conditions (Fig. 3A). Thus, we selected MDA-MB-231 cells, which express high amounts of ALCAMe, to prepare whole cell lysates and performed an affinity chromatography on anti-ALCAM antibody coupled to a modified protein A. BIAcore chips were prepared, thus obtaining an apparent K_D for the interaction of Gal-8 with ALCAMe of 3.19×10^{-6} M by kinetic analysis, which suggested that Gal-8 specifically interacts with ALCAMe (Fig. 1C, Table 1). Nonlinear and kinetic analyses of Gal-8 binding to different forms of human ALCAM were determined by SPR as plots of response versus Gal-8 concentrations: interestingly, ALCAMgly (Fig. 1B) and ALCAMe (Fig. 1D) showed sigmoid plots, suggesting that the interaction between each of those ALCAM molecules and Gal-8 is mediated by two different binding sites or a cooperative phenomenon, while the

Fig. 1. *Surface plasmon resonance analysis of the interaction between ALCAM and Gal-8.* (A) SPR sensorgram showing the interaction of immobilized recombinant glycosylated ALCAM ectodomain (ALCAMgly) (400 resonance units, RU) with Gal-8 (10–0.6 μM). (B) Nonlinear analysis of the interaction Gal-8/ALCAMgly displays a sigmoid plot suggesting a cooperative phenomenon or at least two interaction sites. (C) SPR sensorgram of immobilized endogenous ALCAM (ALCAMe, 400 RU) from human MDA-MB-231 with Gal-8 (4–0.5 μM). (D) The interaction of Gal-8 with ALCAMe from MDA-MB-231 cells showed sigmoid a plot. (E) SPR sensorgram of recombinant human non-glycosylated ALCAM (ALCAMnongly) with Gal-8 (10–0.6 μM). (F) Nonlinear analysis of the interaction Gal-8/ALCAMnongly displayed a hyperbolic curve, which suggests the existence of one interaction site. SPR sensorgrams of ALCAMgly (G, I) or ALCAMe (H, J) with Gal-8-lactose (10–0.15 μM) and Gal-8-TDG (10–0.15 μM), respectively, are shown after correction for the non-specific binding. Gal-8 preincubation with lactose or TDG induced a complete inhibition of lectin binding to immobilized ALCAMgly or ALCAMe, while the non-related sugar sucrose had no effect (data not shown). Under our experimental conditions, Gal-1 and concanavalin A (data not shown) displayed no specific binding to human ALCAMgly, ALCAMnongly, or ALCAMe up to a concentration five times higher than the Gal-8 K_D (2 μM). RU: resonance unit.

Please cite this article as: M.M. Fernández, et al., Glycosylation-dependent binding of galectin-8 to activated leukocyte cell adhesion molecule (ALCAM/CD166) promotes its surface seg..., Biochim. Biophys. Acta (2016), http://dx.doi.org/10.1016/j.bbagen.2016.04.019

Table 2
Differences in sialylation between recombinant ALCAM (ALCAMgly) and endogenous ALCAM from MDA-MB-231 cells (ALCAMe). Proportions of sialic acid linkages were calculated by cleavage with *A. urefaciens* Neuraminidase (Neuraminidase A), which hydrolyzes both α(2,6) and α(2,3) sialic acid or *S. typhymurium* Neuraminidase, specific for α(2,3) sialic acid linkages. Areas were quantified by weak anionic exchange chromatography (WAX-HPLC), based on 2-aminobenzamide-labeled *N*-glycans.

Sample	Disialylated *N*-glycans (%)		Trisialylated *N*-glycans (%)		Percentage of sialylated *N*-glycans by linkage	
	α(2,3)	α(2,6)	α(2,3)	α(2,6)	α(2,3)	α(2,6)
ALCAMe	13	87	66	34	31	69
ALCAMgly	100	ND	100	ND	100	ND

ND: not detected.

recombinant non-glycosylated ALCAM (ALCAMnongly) (Fig. 1F) that we had previously studied [23] displayed a hyperbolic curve, suggesting the existence of one binding site. Pre-incubation of Gal-8 with lactose (a β-galactoside-related saccharide) completely blocked the interaction with ALCAMgly (Fig. 1G) and ALCAMe (Fig. 1H). In the same sense, thiodigalactoside (TDG, another β-galactoside-related saccharide) completely blocked ALCAMgly (Fig. 1I) and ALCAMe (Fig. 1J) interactions with Gal-8, while non-related saccharides like sucrose had no effect (data not shown). Under our experimental conditions, Gal-1 and concanavalin A displayed no specific binding to human ALCAMgly, ALCAMnongly, or ALCAMe up to a concentration five times higher than the Gal-8 K_D (2 μM) (data not shown). In conclusion, endogenous ALCAM from breast cancer cells serves as a specific Gal-8-binding partner, and differently binds to this lectin in a glycan-dependent fashion.

3.2. Differential sialylation between ALCAMgly and ALCAMe causes changes in Gal-8 affinity

The higher affinity for Gal-8 showed by ALCAMgly expressed in HEK-293 cells, when compared to ALCAMe isolated from MDA-MB-231 cells, and the glycan specificity of ALCAM/Gal-8 interactions (demonstrated by lactose and TDG inhibition) led us to analyze the glycosylation profiles in both ALCAM glycoproteins. The *N*-terminal CRD of Gal-8 has high affinity for α(2,3)-sialylated or 3'-sulfated galactosides, which is quite particular among galectins [26,27,47]. Addition of sialic acid in *N*-glycans is performed by specific sialyltransferases (ST3Gal1 and ST6Gal1), transferring this negatively charged monosaccharide with α(2,3) or α(2,6) linkages to glycoproteins. As previously shown, modification with α(2,6)-linked sialic acid blocks Gal-8 binding [47]. Hence, we determined the sialylation profiles in ALCAMgly versus ALCAMe (isolated by affinity chromatography in Gal-8-Affi-Gel 10). Separation of released *N*-glycans from both samples was based on negative charge using WAX-HPLC. This analysis of *N*-glycans showed primarily neutral, di and tri-negatively charged structures in both samples; tetra-negatively charged *N*-glycans were also present but in minor proportion. Complete digestion of all the negatively charged peaks with α(2–3, 6, 8, 9) Neuraminidase A showed absence of sulfated structures in both ALCAMgly and ALCAMe, discarding the presence of sulfated *N*-glycans. Finally, digestion with a specific α(2,3) sialidase exposed a clear difference between the two ALCAM molecules regarding α(2,3) sialylation: ALCAMgly presents mostly α(2,3)-sialylated glycans, demonstrated by complete digestion with this enzyme. On the other hand, ALCAMe has an important percentage of α(2,6)-sialylated glycans, a modification that prevents, at least in part, Gal-8 binding. Results are summarized in Table 2 and Fig. 2.

3.3. Surface ALCAM from breast cancer cells physically interacts with immobilized Gal-8

Next, we performed cell binding assays in SPR, comparing MDA-MB-231 cells that were transduced with ALCAM-specific shRNA lentiviral particles (MDA-MB-231-shALCAM) versus control cells (transduced with scrambled-shRNA lentiviral particles; mock-transduced; MDA-MB-231-shControl cells). Down-regulation of ALCAM mRNA levels in MDA-MB-231-shALCAM was 88.85% versus the corresponding levels in MDA-MB-231 cells (taken as 100%) ($p < 0.001$), as determined by real-time quantitative RT-PCR; the control lentiviral construction carrying scrambled-shRNA used for mock transduction produced a non-statistically significant reduction of ALCAM mRNA level of 13.95% in MDA-MB-231-shControl cells (Fig. 3B, upper panel). ALCAM knockdown in MDA-MB-231-shALCAM versus mock-transduced cells was confirmed by Western blot (75%, Fig. 3B, lower panel). Unfixed MDA-MB-231 cells (500,000/ml) that have been silenced for ALCAM showed reduced binding to immobilized Gal-8 as compared with mock-transduced cells by SPR. Lactose reduced the binding of unfixed mock-transduced MDA-MB-231 cells to Gal-8-treated BIAcore chips (Fig. 3D). T47D cells, which did not express neither total ALCAM in lysates analyzed by Western blot (Fig. 3B, lower panel) nor surface

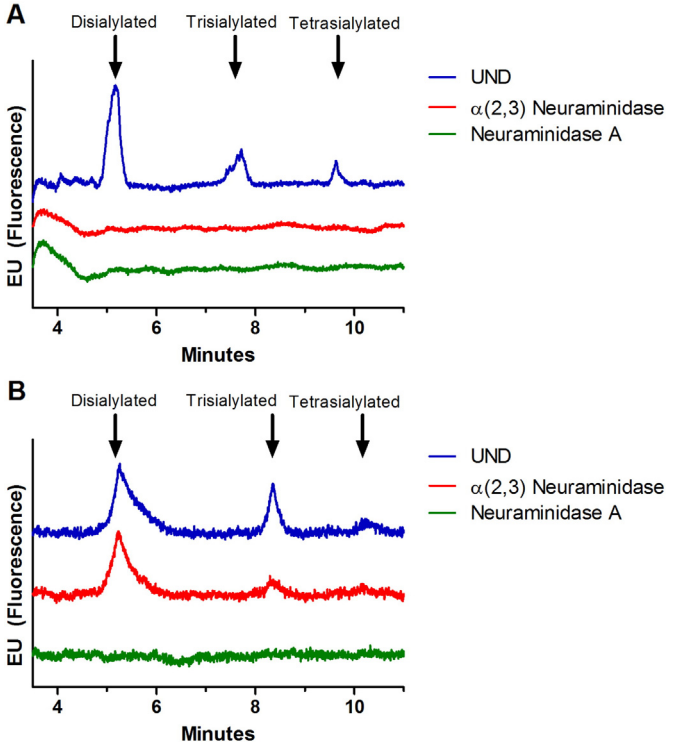

Fig. 2. *WAX-FLR chromatography of released* N*-glycans from (A) recombinantly expressed ALCAM (ALCAMgly) and from (B) endogenous ALCAM from MDA-MB-231 cells (ALCAMe).* *N*-glycan release, 2AB-labeling and WAX chromatography were performed for both samples as described in Materials and methods. Glycans were separated by negative charges, and compared to fetuin *N*-glycans as external standards (arrows). Digestion with *A. urefaciens* sialidase (α(2–3, 6, 8, 9) Neuraminidase A) demonstrated absence of sulfated structures in both samples. (A) ALCAMgly showed complete digestion with a specific α(2,3) Neuraminidase, as expected from a recombinantly expressed glycoprotein in HEK-293 cells. (B) Uncomplete digestion of ALCAMe by α(2,3) *S. typhymurium* Neuraminidase demonstrated an important proportion of α(2,6) sialylation. 2AB: 2-aminobenzamide. EU: emission unit (fluorescence). UND: undigested sample.

ALCAM detected by flow cytometry (Fig. 3C), showed decreased binding to immobilized Gal-8 as compared to mock-transduced MDA-MB-231 cells, as measured by SPR (Fig. 3D). Thus, breast cancer cells bind to extracellular immobilized Gal-8 through specific interactions with cell surface ALCAM.

3.4. Soluble extracellular Gal-8 binds to the breast cancer cell surface

To analyze Gal-8 secretion from breast cancer cells, we evaluated conditioned media compared to lysates from MDA-MB-231 cells by Western blot (Fig. 4A). The full-length transmembrane ALCAM

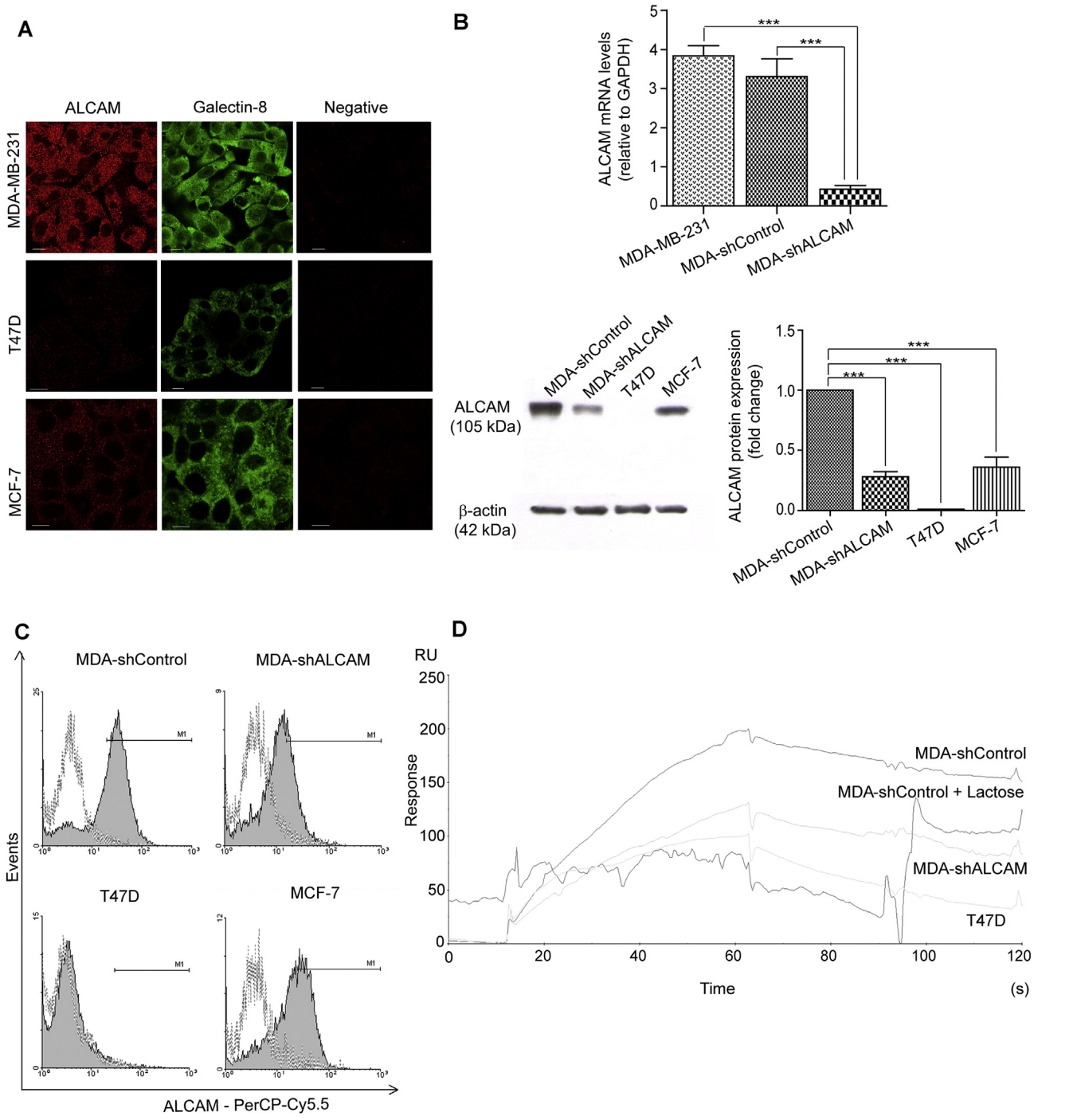

Fig. 3. *Surface ALCAM from breast cancer cells interacts with Gal-8 in a glycan-dependent fashion.* (A) Indirect immunofluorescence for ALCAM and Gal-8 expression in permeabilized MDA-MB-231, T47D, and MCF-7 breast cancer cells, by confocal microscopy. (B) Upper panel: The bar graph shows real-time quantitative RT-PCR analysis of ALCAM mRNA levels in MDA-MB-231-shALCAM (MDA-shALCAM) cells versus the corresponding levels in MDA-MB-231 and mock-transduced MDA-MB-231 (MDA-shControl) cells, normalized by using GAPDH: MDA-shALCAM cells showed 88.85% of ALCAM silencing versus MDA-MB-231 cells (taken as 100%) ($p < 0.001$). Lower panels: Western blot analysis was also performed to study ALCAM protein levels in whole lysates from MDA-shControl, MDA-shALCAM, T47D, and MCF-7 breast cancer cells; lysates were run in parallel in the same 10% gel in SDS-PAGE, and then electrotransferred onto PVDF. Blots were probed with the anti-ALCAM monoclonal antibody, followed by the incubation with the secondary antibody conjugated to HRP and detection by chemiluminiscence. Densitometric analysis of β-actin was used to normalize the protein loading in order to compare ALCAM levels. Data were analyzed by Student's *t*-test ($^{***}p < 0.001$). (C) Flow cytometry analysis of surface ALCAM expression in non-permeabilized MDA-shControl, MDA-shALCAM, T47D, and MCF-7 breast cancer cells. (D) SPR sensorgrams showing the interactions of immobilized Gal-8 (400 RU) in BIAcore chips with MDA-shControl, MDA-shALCAM, and T47D breast cancer cells. The interaction of mock-transduced MDA-shControl cells with immobilized Gal-8 was inhibited by 20 mM lactose. RU: resonance unit.

Please cite this article as: M.M. Fernández, et al., Glycosylation-dependent binding of galectin-8 to activated leukocyte cell adhesion molecule (ALCAM/CD166) promotes its surface seg..., Biochim. Biophys. Acta (2016), http://dx.doi.org/10.1016/j.bbagen.2016.04.019

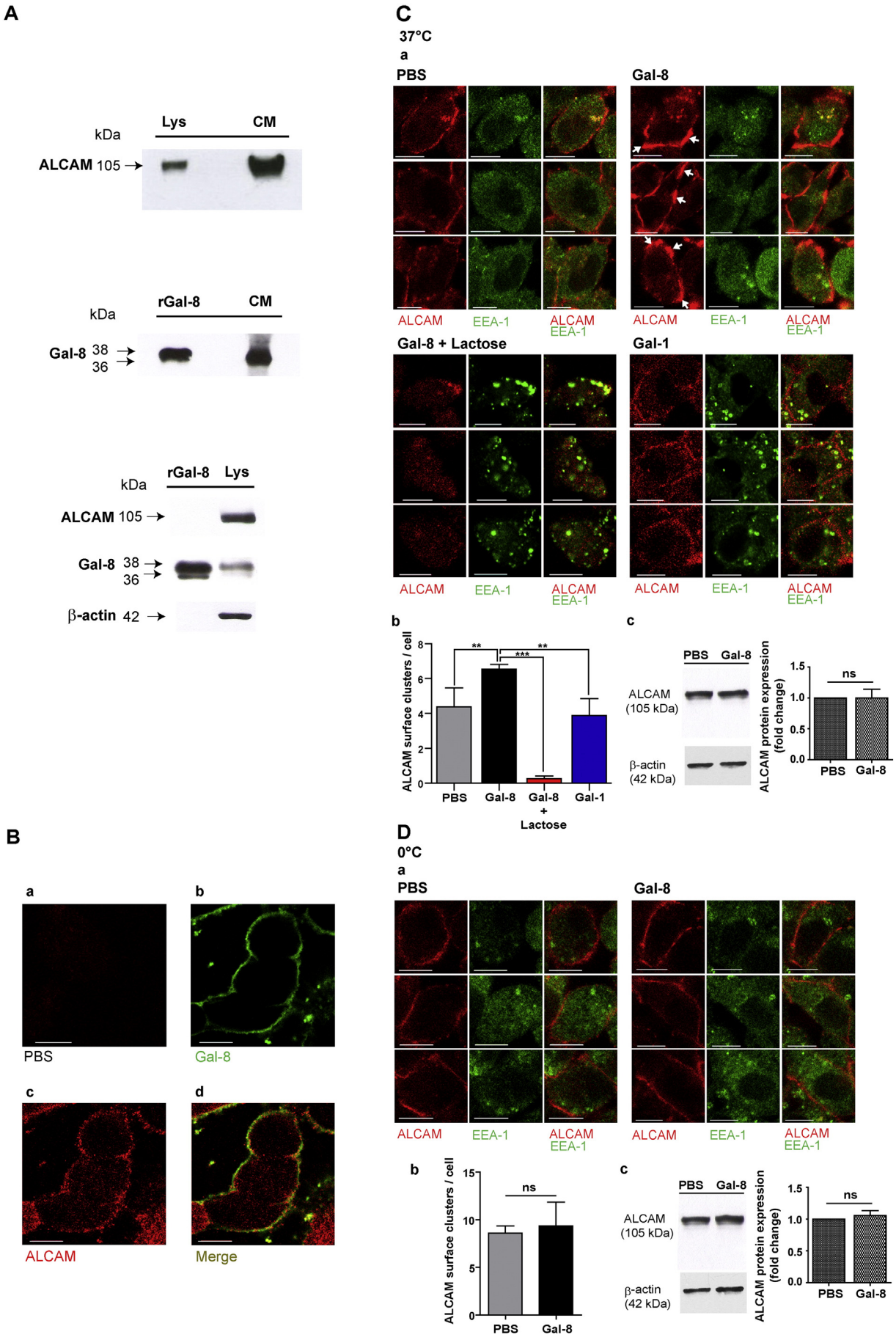

Please cite this article as: M.M. Fernández, et al., Glycosylation-dependent binding of galectin-8 to activated leukocyte cell adhesion molecule (ALCAM/CD166) promotes its surface seg..., Biochim. Biophys. Acta (2016), http://dx.doi.org/10.1016/j.bbagen.2016.04.019

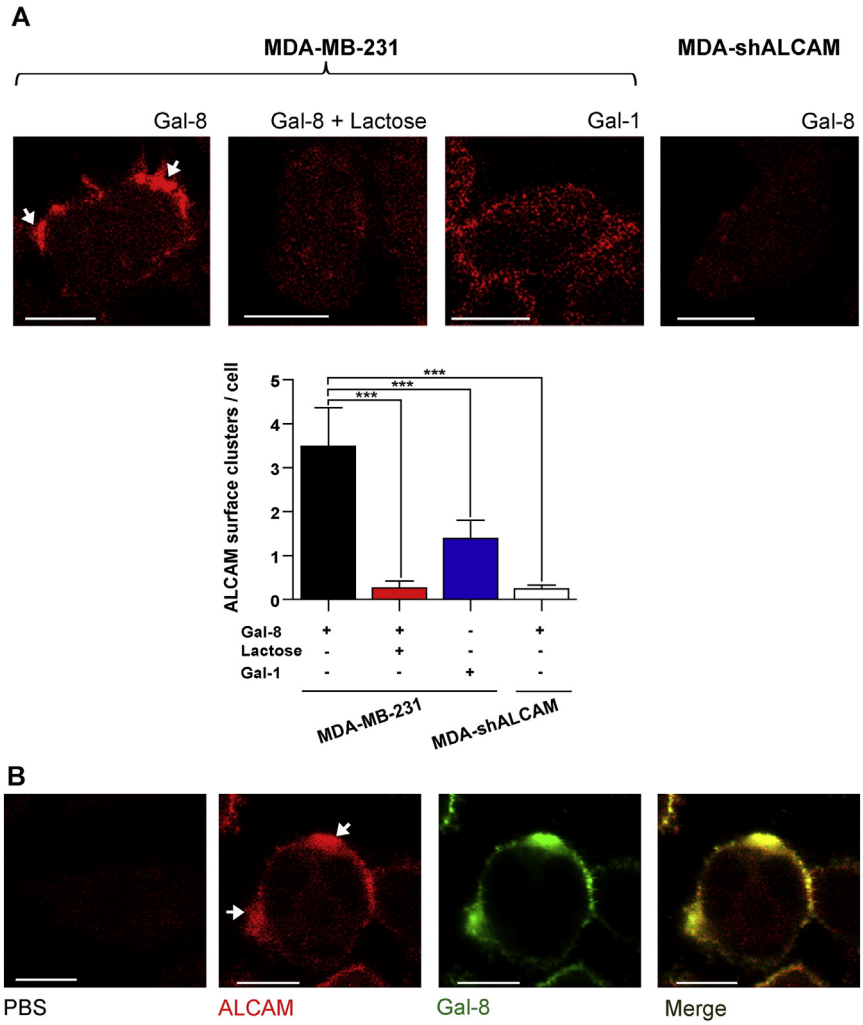

Fig. 5. *ALCAM surface clusters induced by Gal-8 are prevented by receptor silencing, and show colocalization with Gal-8 in MDA-MB-231 breast cancer cells.* (A) Confocal microscopy of ALCAM internalization in MDA-MB-231 cells pre-treated with Gal-8, Gal-8 in the presence of lactose or Gal-1, and in MDA-MB-231-shALCAM (MDA-shALCAM) cells pre-treated with Gal-8. Cells were incubated with anti-ALCAM-PerCP-Cy5.5 for 2 h on ice, and internalization was conducted at 37 °C for 10 min. One representative confocal image of ALCAM staining (red) is shown for each treatment or cell type, from three independent experiments. MDA-shALCAM cells pre-treated with Gal-8 did not show ALCAM segregation at the surface, after incubation at 37 °C for 10 min. White arrows indicate receptor segregation in the presence of Gal-8. The bar graph displays membranous ALCAM cluster quantification as determined by Imaris 3D software. (B) Immunofluorescence staining for Gal-8 in Gal-8-treated MDA-MB-231 cells after internalization at 37 °C for 30 min. ALCAM clusters display colocalization with Gal-8 (Manders' colocalization coefficient = 0.79 ± 0.07, according to [49]). ALCAM was stained with anti-ALCAM-PerCP-Cy5.5 (red) and Gal-8 was stained with the primary antibody followed by Alexa Fluor 488-conjugated secondary antibody (green). Magnification bars: 10 μm.

(105 kDa) was detected in MDA-MB-231 cell lysates as expected (Fig. 4A, upper and lower panel) while a soluble ALCAM molecule of slightly lower molecular weight was observed in conditioned media (Fig. 4A, upper panel). Gal-8 was detected in lysates from MDA-MB-231 cells as two protein bands of ~38 and ~36 kDa (probably corresponding to endogenous isoforms; Fig. 4A, lower panel) and as a broad band of similar MW in the conditioned media (Fig. 4A, middle panel). These results showed that MDA-MB-231 cells secrete Gal-8 to

Fig. 4. *Extracellular Gal-8 induces ALCAM segregation at the surface of MDA-MB-231 breast cancer cells.* (A) Immunoblot analysis of extracellular and intracellular ALCAM and Gal-8 in MDA-MB-231 cells. Conditioned media and whole extracts were evaluated. The full-length transmembrane ALCAM (105 kDa) was detected in MDA-MB-231 cell lysates (upper and lower panel) while a soluble ALCAM molecule of slightly lower molecular weight was observed in the conditioned media (upper panel). Gal-8 was detected in lysates from MDA-MB-231 cells as two protein bands of ~38 and ~36 kDa (lower panel) and as a broad band of similar MW in conditioned media (middle panel). A representative immunoblot is shown for each sample. Lys: cell lysates. CM: conditioned medium after 48 h incubation. rGal-8: recombinant Gal-8, which is observed as a double band (with and without a *c-myc* tag). (B) Cell surface expression of endogenous ALCAM and surface labeling with exogenous recombinant Gal-8 in MDA-MB-231 cells, as evaluated by confocal microscopy. Endogenous ALCAM was developed with an unconjugated anti-ALCAM monoclonal antibody followed by Alexa 555-conjugated secondary antibody (red). Exogenous Gal-8 was added and detected with the anti-Gal-8 primary antibody followed by Alexa 488-conjugated secondary antibody (green). Each experiment was performed three times with reproducible results. Magnification bars: 10 μm. (C) (a) Confocal microscopy of ALCAM internalization in MDA-MB-231 cells pre-treated with PBS or Gal-8 for 30 min on ice (upper panels). Cells were then incubated with a monoclonal antibody anti-ALCAM conjugated to PerCP-Cy5.5 for 2 h on ice. Internalization was induced at 37 °C for 30 min. Cells were fixed, permeabilized, and probed with anti-EEA1 primary antibody to visualize early endosomes (green). Three representative confocal images are shown, and ALCAM (red), EEA1 (green), and merged staining are illustrated for each image. White arrows indicate receptor segregation in the presence of Gal-8. Lactose treatment before Gal-8 incubation and replacement of Gal-8 by Gal-1 (in the absence of lactose) are also shown (lower panels). (b) The bar graph shows membranous ALCAM cluster quantification per cell, excluding intracellular spots, by using Imaris 3D software when internalization was conducted at 37 °C for 30 min; values represent the mean ± S.D., as analyzed by Student's *t*-test ($^{*}p < 0.025$). (c) Western blot analysis of whole cell lysates from Gal-8-treated versus PBS-treated cells after the internalization assay at 37 °C for 30 min: Gal-8 treatment did not modify total ALCAM protein levels. (D) (a) Confocal microscopy for ALCAM in MDA-MB-231 cells pre-treated with PBS or Gal-8 as in (C), after blocking the internalization at 0 °C. Three representative confocal images are shown, and ALCAM (red), EEA1 (green), and merged staining are illustrated for each image. (b) The bar graph shows membranous ALCAM cluster quantification per cell, after blocking the internalization at 0 °C, as determined by Imaris 3D software. (c) Western blot analysis of whole cell lysates from Gal-8-treated versus PBS-treated cells after treatment at 0 °C for 30 min: Gal-8 treatment did not modify total ALCAM protein levels. Magnification bars: 10 μm. ns: not statistically significant results.

Please cite this article as: M.M. Fernández, et al., Glycosylation-dependent binding of galectin-8 to activated leukocyte cell adhesion molecule (ALCAM/CD166) promotes its surface seg..., Biochim. Biophys. Acta (2016), http://dx.doi.org/10.1016/j.bbagen.2016.04.019

the extracellular milieu, as described for other galectins. To evaluate cell surface binding of exogenously added Gal-8, we incubated non-permeabilized MDA-MB-231 cells with recombinant Gal-8 followed by immunofluorescence staining for Gal-8 and ALCAM. As shown in Fig. 4B, Gal-8 bound to putative ligands at the cell surface. Importantly, the yellow merged fluorescence observed for ALCAM and Gal-8 double staining suggested that both molecules co-localized at least partially around the cell surface. As expected, ALCAM showed immunostaining at the surface of MDA-MB-231 cells (Fig. 4B). Therefore, exogenously added soluble Gal-8 binds to the surface of MDA-MB-231 cells and co-localizes at least partially with ALCAM.

3.5. Gal-8 induces ALCAM segregation at the surface of MDA-MB-231 breast cancer cells

Internalization of ALCAM was induced by treating MDA-MB-231 cells with the anti-ALCAM-PerCP-Cy5.5 monoclonal antibody on ice in the presence or absence of exogenous recombinant Gal-8, followed by an incubation at 37 °C for 0–60 min. In Gal-8-treated cells, we found ALCAM segregation at several regions of the cell surface after incubation at 37 °C, as observed by confocal microscopy (Fig. 4C.a, white arrows). Membranous ALCAM clusters per cell were quantified from confocal images as a measure of receptor segregation by using Imaris 3D software 6.3.1 (Bitplane Sci. Software, Zürich, Switzerland) as previously described [48], detecting increased number of ALCAM spots at the surface of Gal-8-treated versus PBS-treated cells incubated at 37 °C ($p < 0.025$) (Fig. 4C.b). Lactose pre-treatment blocked the effect of exogenously added Gal-8 on MDA-MB-231 cells, and moreover, it is supposed to remove endogenous Gal-8 (and other galectins) bound to the cell surface (Fig. 4C.a and b). Gal-1, which in SPR measurements showed no binding to ALCAM up to a lectin concentration of 10 μM, did not significantly modify the number of ALCAM surface clusters in lectin-treated versus PBS-treated cells incubated at 37 °C when used at 4–8 μM (Fig. 4C.a and b). Gal-8 effect was prevented when cells were incubated on ice (Fig. 4D.a and b). To examine if Gal-8 treatment can modify total ALCAM protein levels, we performed Western blot analysis of whole cell lysates from Gal-8-treated versus PBS-treated cells after the internalization assay at 37 °C for 30 min (Fig. 4C.c): Gal-8 treatment did not modify total ALCAM protein levels, which was also verified when the same assays were performed at 0 °C for 30 min (Fig. 4D.c). MDA-MB-231-shALCAM cells (Fig. 5A) did not show ALCAM segregation when they were exogenously treated with Gal-8 and incubated at 37 °C, calculated as the number of membranous ALCAM clusters per cell by Imaris 3D, as compared with Gal-8-treated MDA-MB-231 cells ($p < 0.001$). Moreover, MDA-MB-231-shALCAM cells treated with Gal-8 showed increased —although faint— cytoplasmic density of ALCAM-positive spots as compared with Gal-8-treated MDA-MB-231 cells (Fig. 5A) when incubation was performed at 37 °C, probably suggesting that ALCAM silencing diminished Gal-8-induced ALCAM retention at the cell surface and therefore increased ALCAM internalization. As shown in Fig. 4C.a, lactose addition in the presence of exogenous Gal-8 blocked ALCAM segregation at the surface of MDA-MB-231 cells incubated at 37 °C (Fig. 5A). Gal-1 (8 μM) treatment yielded a low number of ALCAM clusters per cell at the surface of MDA-MB-231 cells as compared with Gal-8-treated cells when incubated at 37 °C (Fig. 5A). Next, we analyzed if ALCAM surface clusters showed colocalization with Gal-8 in MDA-MB-231 cells that were treated with exogenous Gal-8 and incubated at 37 °C. Thus, we performed the immunofluorescence staining for Gal-8, detecting Gal-8 colocalization (Manders' colocalization coefficient = 0.79 ± 0.07, according to [49]) with ALCAM at the surface clusters, which indicated a direct effect of Gal-8 on surface ALCAM cross-linking (Fig. 5B). In conclusion, addition of exogenous Gal-8 induced glycosylation-dependent ALCAM segregation at the surface of MDA-MB-231 cells, inducing ALCAM cross-linking.

3.6. ALCAM and Gal-8 are widely expressed in vivo in human breast tissues

In order to evaluate co-expression of ALCAM and Gal-8 in human breast tissues, we analyzed both molecules by immunohistochemistry on paraffin-embedded archival specimens from human primary ductal breast carcinomas and normal tissues. Three groups of samples from normal, DCIS, and IDC tissues were analyzed. Table 3 summarizes clinical and pathological parameters of patients. Immunohistochemistry for ALCAM revealed strong staining at the intercellular junctions in the plasma membrane of epithelial cells from normal tissues and DCIS, but weaker cytoplasmic staining ($p < 0.05$, n = 10/group). In IDC, we observed less membranous and increased cytoplasmic staining for ALCAM ($p < 0.05$), as compared to normal and DCIS tissues (Fig. 6). Regarding Gal-8, this lectin was localized in the nucleus and cytoplasm of epithelial cells in breast tissues. High levels of Gal-8 staining were

Table 3
Clinical and pathological parameters of patients.

Histologic type	Histologic grade	T	N	ER status	PR status	Her2	Margins
Ductal carcinoma *in situ*	G3	pT2	pN0	0	0	ND	Negative
	G2	pT2	pN0	80% (++++)	80% (++++)	ND	Negative
	G1	pT1b	pN0	80% (++++)	75% (+++)	ND	Negative
	G3	pT1	pN0	70% (+++)	90% (++++)	ND	Negative
	G3	pT2	pN0	0	0	ND	Positive
	G3	pT3	pN0	70% (+++)	70% (+++)	ND	Negative
	G2	pT1b	pN0	80% (++++)	80% (++++)	ND	Negative
	G2	pT1c	pN0	90% (+++)	35%	ND	Negative
							Negativo
	2	pT1c	pN0	35% (++)	0	ND	Negative
	G2	pT1c	pN0	75% (+++)	75% (+++)	ND	Negative
Invasive ductal carcinoma	G2	pT2	pN2a	0	30% (++)	Negative (0)	Negative
	G2	pT1c	pN1a	90% (++++)	70% (+++)	Negative (0)	Negative
	G3	pT1b	pN1a	0	0	Positive (3+)	Negative
	G3	pT2(m)	pN2a	0	0	Negative (1+)	Negative
	G2	pT2	pN1a	40% (++)	40% (++)	Negative (1+)	Negative
	G1	pT1b	pN1a	75% (+++)	65% (+++)	Negative (0)	Negative
	G1	pT1b	pNx	70% (+++)	10% (+)	Negative (1+)	Negative
	G2	pT1c	pN1a	60% (+++)	40% (++)	Negative (0)	Negative
	G2	pT1	pN1a	70% (+++)	90% (++++)	Negative (1+)	Negative
	G3	pT2	pN2a	0	0	Negative (0)	Positive

G (histologic grade): assigned according to Nottingham Histologic Score. *pT (size), N (nodes)*: assigned according to TNM Pathologic Staging, College of American Pathologists (CAP), based on the American Joint Committee on Cancer (AJCC/UICC) [80]. *ER (estrogen receptor), PR (progesterone receptor)*: quantified by using both intensity and percentage of positive cells, according to the Allred Score. *Her2 (human epidermal growth factor receptor 2)*: quantified according to American Society of Clinical Oncology–College of American Pathologists (ASCO-CAP), Clinical Practice Guideline Update, 2013 [81]. ND: not determined.

Please cite this article as: M.M. Fernández, et al., Glycosylation-dependent binding of galectin-8 to activated leukocyte cell adhesion molecule (ALCAM/CD166) promotes its surface seg..., Biochim. Biophys. Acta (2016), http://dx.doi.org/10.1016/j.bbagen.2016.04.019

detected in the nuclei of epithelial cells from normal breast tissues and DCIS, which decreased with tumor progression ($p < 0.05$) (Fig. 6). Gal-8-positive immunolabeling in the cytoplasm of epithelial cells from normal tissues and DCIS showed a tendency to decrease in IDC, although this effect did not reach statistical significance (Fig. 6). Moreover, human sera were biochemically analyzed by Western blot to detect ALCAM and Gal-8. A circulating ALCAM protein with slightly smaller molecular weight (~95 kDa) than the full-length ALCAM was detected in human sera, although we could not find significant differences between serum levels of ALCAM in control versus IDC patients. Circulating Gal-8 was also identified by Western blot as a conspicuous band in a ~1:1.4 ratio ($p < 0.05$) in control versus IDC patient sera, respectively (data not shown). In conclusion, our results demonstrate that both ALCAM and Gal-8 are present *in vivo* in human breast tissues and sera, suggesting that they could specifically interact via a glycan-dependent pathway to modulate cancer progression.

4. Discussion

Distinct binding sites in the ALCAM molecule have been involved in homophilic [50] and heterophilic [51] interactions. It has been previously described that homophilic ALCAM interactions show around 100-fold lower affinity (K_D: 29–48 $\times$ 10^{-6} M) than heterophilic interactions with CD6 (K_D: 0.4–1.0 $\times$ 10^{-6} M) [52,53], being the latter affinity similar to the one measured in the present study for the ALCAM/Gal-8 heterophilic interactions. Herein, by SPR, we compared the ability of Gal-8 to bind to the human glycosylated ALCAM ectodomain (ALCAMgly) or to the endogenous ALCAMe isolated from MDA-MB-231 cells. We found that both ALCAM molecules can interact *in vitro* with Gal-8 in a glycan-dependent manner, as expected because ALCAM has been previously identified as a glycoprotein with 10 *N*-glycosylation sites [4,54]. Recombinant ALCAMgly showed higher binding affinity to Gal-8 (K_D: 1.09 x 10^{-7} M; kinetic analysis) than ALCAMe (K_D: 3.19 $\times$ 10^{-6}°M; kinetic analysis), as detected by SPR. Importantly, our findings suggest that ALCAMe glycoforms actually interact with recombinant Gal-8 in SPR, and these associations are specifically inhibited by β-galactoside derivatives. In previous studies, we reported the interaction of Gal-8 with a non-glycosylated form of human recombinant ALCAM (ALCAMnongly): notably, Gal-8 binding was also inhibited by β-galactoside derivatives, suggesting that there could be protein-protein interactions with ALCAM at or close to the galectin CRD [23]. When kinetic analysis of Gal-8 binding to different ALCAM molecules was performed, the main differences

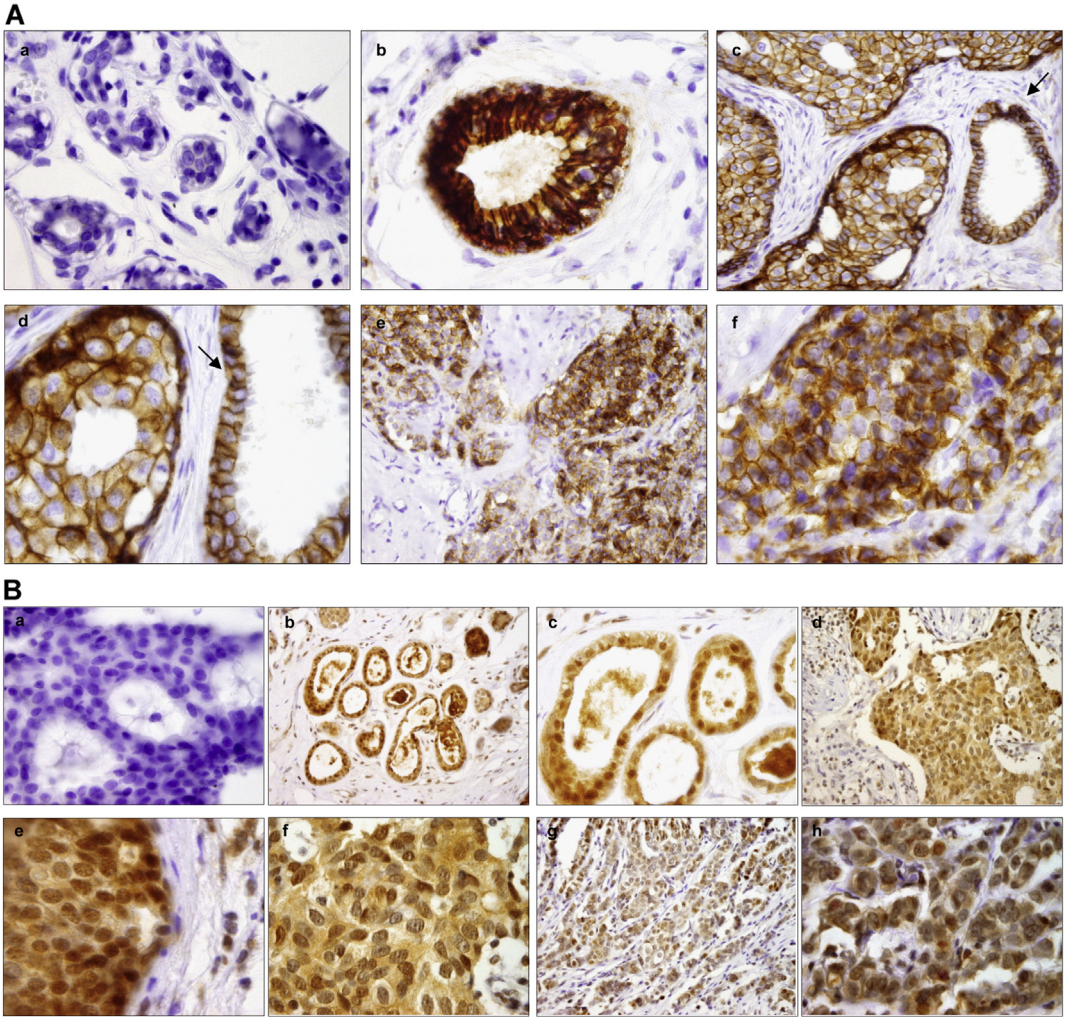

Fig. 6. *ALCAM and Gal-8 are co-expressed in normal and malignant human breast tissues.* Archival paraffin-embedded specimens from human breast tissues were processed for immunohistochemical staining. (A) Immunohistochemistry for ALCAM: (a) Negative control omitting the primary antibody in normal tissues, showing counterstaining with hematoxylin (×100). (b) Normal breast tissues (×100). (c) Ductal carcinoma *in situ* (×40); the arrow indicates a normal duct. (d) Ductal carcinoma *in situ* (×100); the arrow indicates a normal duct. (e) Invasive ductal carcinoma (×40). (f) Invasive ductal carcinoma (×100). (B) Immunohistochemistry for Gal-8: (a) Negative control in a ductal carcinoma *in situ* (×100). (b) Normal breast tissues (×40). (c) Normal breast tissues (×100). (d) Ductal carcinoma *in situ* (×40). (e, f) Ductal carcinoma *in situ* (×100). (g) Invasive ductal carcinoma (×40). (h) Invasive ductal carcinoma (×100). All sections were stained in parallel without primary antibodies to provide negative controls (data not shown). Representative images for immunohistochemical staining are shown. Experiments were performed three times with reproducible results.

Please cite this article as: M.M. Fernández, et al., Glycosylation-dependent binding of galectin-8 to activated leukocyte cell adhesion molecule (ALCAM/CD166) promotes its surface seg..., Biochim. Biophys. Acta (2016), http://dx.doi.org/10.1016/j.bbagen.2016.04.019

between K_Ds were due to the association rate or *kon*: the interaction ALCAMgly/Gal-8 was characterized by a *kon* of 2.32×10^4 $(M.s)^{-1}$, while ALCAMnongly/Gal-8 interaction displayed a one order of magnitude lower *kon* of 3.29×10^3 $(M.s)^{-1}$; the dissociation rates or *koff* for both interactions remained within the same order of magnitude. However, the *kon* for the interaction ALCAMe/Gal-8 was maintained at the same order of magnitude than the one calculated for the complex ALCAMgly/Gal-8, although the K_D value was close to the one previously reported for ALCAMnongly/Gal-8 interaction [23]. Taken together, our results suggest that the interactions between ALCAM and Gal-8 are modulated by specific carbohydrates, and probably mediated by protein–glycan and protein–protein interactions at different binding sites. Sialylation profiling by WAX chromatography showed clear differences between ALCAMgly and ALCAMe: both samples lacked sulfated *N*-glycans, as demonstrated by complete digestion of negatively charged *N*-glycans by *A. urefaciens* sialidase. This result discarded the possibility of differences in 3′-sulfated lactosamine structures that would bind Gal-8 with high affinity. ALCAMgly and ALCAMe presented a similar WAX profile, with major proportions of neutral, di-, and tri-sialylated *N*-glycans. However, ALCAMgly sialylated *N*-glycans were almost completely α(2,3)-sialylated (if present, levels of α(2,6) sialylation were less than 1%), in opposition to ALCAMe, where α(2,6) sialylation was prominent (approximately 69% of α(2,6) sialylation when areas from di- and tri-sialylated *N*-glycans were combined). These observations are consistent with previous reports [55], demonstrating that HEK-293 cells express very low endogenous levels of ST6Gal-I activity, the sialyltransferase responsible for the α(2,6) sialic acid addition. In contrast, MDA-MB-231 cell surface glycoconjugates were shown to be highly α(2,6)-sialylated by selective detection of sialic acid linkage on the cell surface using plant lectins and sialidase hydrolysis [56]. The presence of higher levels of α(2,6) sialic acid in *N*-glycans is then responsible for the described lower affinity of Gal-8 for ALCAMe from MDA-MB-231 cells. This Gal-8 preference for α(2,3)-sialylated glycans has also been described for β1 integrins in trabecular meshwork [47].

It should be pointed out that Escoda–Ferran and coworkers demonstrated ALCAM/Gal-1 interactions by ELISA, but the K_D of this association has not been reported [57]. In fact, we found no specific interaction between ALCAM and Gal-1 by SPR up to 10 μM Gal-1, although we could not discard a specific ALCAM/Gal-1 interaction at higher concentrations of the lectin, which suggests a lower affinity than the one calculated for ALCAM/Gal-8 interactions. Interestingly, the sialylation levels detected in ALCAMe from MDA-MB-231 cells explained the low affinity displayed by Gal-1 in SPR experiments, as α(2,6) sialylation is also restrictive for Gal-1 binding, while α(2,3) sialylation allows Gal-1 binding but with lower affinity [58]. Current efforts are aimed at examining the complete *N*-glycan profile of both ALCAMgly and ALCAMe, in order to further understand the mechanisms of selectivity for Gal-8 binding. Moreover, endogenous ALCAM from MDA-shControl cells (Fig. 3A) could be more prominently glycosylated than ALCAM expressed by MCF-7 cells as a broad protein band could be detected by Western blot analysis of these cells. Although *N*-glycosylation of ALCAM from MCF-7 cells has not yet been characterized, this effect might explain differential *in vivo* tumorigenicity and metastatic potential.

Extracellular lectin-glycan interactions function by trapping glycoprotein receptors at the cell surface, preventing their endocytosis and modulating cell signaling [59–61]. These lectin-glycoprotein complexes have been well documented, for example in the case of Gal-3/CD45/TCR [62], Gal-1/CD45 [63], Gal-1/VEGFR2 [64], and Gal-3/N-cadherin interactions [65]. For instance, Gal-3 has been proposed to form clusters with glycosylated growth factor receptors at the cell surface that inhibit constitutive endocytosis and prolong downstream signaling, thereby promoting cell proliferation and survival [66,67]. Although ALCAM endocytosis has been previously reported [19,20], here we showed that Gal-8 induces ALCAM segregation at the surface of MDA-MB-231 breast cancer cells, possibly trapping membranous ALCAM and preventing its internalization. Importantly, herein, we demonstrated that Gal-8 is secreted from breast cancer cells to the conditioned media, which favors the hypothesis of the interaction between extracellular Gal-8 and membranous ALCAM at the cell surface. Thus, secreted Gal-8 might act as an autocrine or paracrine regulator of ALCAM signaling in breast cancer cells. Regarding soluble ALCAM, a glycosylated ~96–100 kDa form of ALCAM has been described in the conditioned media from different cell types [21,22,68]. In fact, ADAM17 has been discovered to be an important proteolytic sheddase of ALCAM [21], a mechanism that can enhance tumor cell motility and migration [22]. Herein, by Western blot, we found a soluble ALCAM form in MDA-MB-231 cell conditioned media of slightly lower molecular weight than the whole molecule (105 kDa), which seems to correspond to the previously described glycosylated ectodomain [21,22].

In order to explore the occurrence of the ALCAM/Gal-8 axis in human tissues, we studied the *in vivo* expression of ALCAM and Gal-8 in normal breast and ductal carcinoma (the most common histological subtype of mammary tumor) specimens by immunohistochemistry. Regarding the cell adhesion molecule ALCAM in breast cancer, its high cytoplasmic expression has been associated with higher tumor grading [17] and lower disease-free survival [17,69]. Tissue microarray studies demonstrated that ALCAM is usually expressed in normal and cancerous breast epithelium, and that a marked reduction of ALCAM expression characterizes patients with poor clinical outcome [70]. Low expression of ALCAM at sites of cell–cell contact in primary breast tumors has been proposed to contribute to a more aggressive phenotype [71]. Regarding Gal-8, this lectin has been previously reported in benign breast tissues and lobular breast carcinomas [40], and it has also been identified as one of the five most frequently expressed tumor antigens in a transgenic mouse model of breast cancer (epidermal growth factor receptor 2 (HER2-neu)-positive and estrogen receptor (ER)-negative) [72]. Gal-8 expression seems to differ depending on the type of human mammary tumor, as analyzed by gene expression microarrays: basal-like breast cancer showed lower Gal-8 expression as compared with luminal B tumors, while HER2-neu-positive breast cancer showed the highest Gal-8 expression (in accordance with [72]); moreover, patients with higher levels of Gal-8 transcripts showed better relapse-free survival [73]. Herein, we provide compelling evidences of the co-occurrence of ALCAM and Gal-8 in human mammary epithelium, which enables us to speculate that the physical interaction that we demonstrated *in vitro* might also take place *in vivo* in breast tissues. We also detected prominent membranous ALCAM expression in normal and DCIS tissues, which diminished in IDC, suggesting altered ALCAM homophilic interactions at the cell surface in IDC. As far as we know, ALCAM/Gal-8 interactions have not been studied elsewhere, and their potential roles at the site of the primary tumor or at the metastatic site are unknown. From a functional standpoint, Gal-8/ALCAM interactions may play a role in tumor angiogenesis [23], migration [30], and cancerous osteolysis due to metastasis [74], but it may also play a possible role in tumor-immune escape given the recent findings that Gal-8 promotes expansion of regulatory T cells through modulation of TGF-β and IL-2 signaling [75]. Regarding epithelial-to-mesenchymal transition (EMT) and ALCAM homophilic or heterophilic interactions, for example in pancreatic cancer progression, the level of Zeb1 mRNA —an EMT activator— has been found greater in $CD166^-$ cells than that in $CD166^+$ cells, suggesting that ALCAM silencing might be involved in EMT [76]. Although there is still no evidence of the role of Gal-8 as a potential inducer of EMT, future studies should explore this possibility given the involvement of other galectin family members in this process [77–79]. In conclusion, the ALCAM/Gal-8 heterophilic interaction at the cell surface could also act by regulating ALCAM-ALCAM intercellular contacts in breast tissues, thereby modulating cellular cohesion in physiological conditions and/or cell dissemination and metastasis in neoplastic settings.

5. Conclusion

In summary, our results support the occurrence of heterophilic interactions of ALCAM with Gal-8 at the surface of breast cancer cells.

Please cite this article as: M.M. Fernández, et al., Glycosylation-dependent binding of galectin-8 to activated leukocyte cell adhesion molecule (ALCAM/CD166) promotes its surface seg..., Biochim. Biophys. Acta (2016), http://dx.doi.org/10.1016/j.bbagen.2016.04.019

Specific interactions between endogenous ALCAM from breast cancer cells and recombinant Gal-8 are demonstrated, which were successfully prevented by β-galactoside-related carbohydrates. Likewise, ALCAM-silenced breast cancer cells show reduced binding to immobilized Gal-8 relative to control cells. Moreover, Gal-8 induces ALCAM segregation at the surface of breast cancer cells, probably trapping membranous ALCAM and delaying its internalization. Co-expression of ALCAM and Gal-8 in human normal breast tissues and ductal carcinomas allowed us to postulate the potential biological role underlying this heterophilic interaction. We hypothesized that the Gal-8/ALCAM axis is active in breast tissues, and that the interaction between extracellular Gal-8 and membranous ALCAM occurs at the surface of breast cells, thereby influencing cell–cell and cell–matrix interactions during health and tumor progression. Further studies are needed to elucidate the fine nature and physiologic relevance of ALCAM/Gal-8 interactions, the influence of different ALCAM glycosylation patterns and the mechanisms and signaling pathways affected.

Conflict of interest

The authors declare no competing financial interest in relation to the work described.

Transparency document

The Transparency document associated with this article can be found, in the online version.

Acknowledgments

M.M.F., M.T.E., M.F.T., M.V.E., C.B., C.W.-T., K.V.M., E.L.M., and G.A.R. are researchers from the Consejo Nacional de Investigaciones Científicas y Técnicas (CONICET), Argentina. F.F. is a fellow from the Agencia Nacional de Promoción Científica y Tecnológica (ANPCyT), Argentina. A.J.C. and L.G.M. are fellows from CONICET. Authors are in debt with Alejandra Trinchero for helpful assistance.

This work was supported by grants from the Agencia Nacional de Promoción Científica y Tecnológica (ANPCyT) [PICT-2012-0071 to M.T.E.; PICT-2010-1333 to M.M.F.], and the Consejo Nacional de Investigaciones Científicas y Técnicas (CONICET) [PIP 2012-2014-382 to M.M.F.; PIP 2012-2014-493 to C.W.-T.]. G.A.R and K.V.M acknowledge support from Sales, Bunge & Born, and René Baron Foundations.

References

[1] A.G. Hansen, G.W. Swart, A. Zijlstra, ALCAM: basis sequence: mouse, AFCS Nat. Mol. Pages 2011 (2011), http://dx.doi.org/10.1038/mp.a004126.004101.
[2] G.W. Swart, P.C. Lunter, J.W. Kilsdonk, L.C. Kempen, Activated leukocyte cell adhesion molecule (ALCAM/CD166): signaling at the divide of melanoma cell clustering and cell migration? Cancer Metastasis Rev. 24 (2005) 223–236.
[3] W.G. Degen, L.C. van Kempen, E.G. Gijzen, J.J. van Groningen, Y. van Kooyk, H.P. Bloemers, G.W. Swart, MEMD, a new cell adhesion molecule in metastasizing human melanoma cell lines, is identical to ALCAM (activated leukocyte cell adhesion molecule), Am. J. Pathol. 152 (1998) 805–813.
[4] U.H. Weidle, D. Eggle, S. Klostermann, G.W. Swart, ALCAM/CD166: cancer-related issues, Cancer Genomics Proteomics 7 (2010) 231–243.
[5] A.G. Hansen, S.A. Arnold, M. Jiang, T.D. Palmer, T. Ketova, A. Merkel, M. Pickup, S. Samaras, Y. Shyr, H.L. Moses, S.W. Hayward, J.A. Sterling, A. Zijlstra, ALCAM/CD166 is a TGF-beta-responsive marker and functional regulator of prostate cancer metastasis to bone, Cancer Res. 74 (2014) 1404–1415.
[6] G. Kristiansen, C. Pilarsky, C. Wissmann, S. Kaiser, T. Bruemmendorf, S. Roepcke, E. Dahl, B. Hinzmann, T. Specht, J. Pervan, C. Stephan, S. Loening, M. Dietel, A. Rosenthal, Expression profiling of microdissected matched prostate cancer samples reveals CD166/MEMD and CD24 as new prognostic markers for patient survival, J. Pathol. 205 (2005) 359–376.
[7] S. Davies, W.G. Jiang, ALCAM, activated leukocyte cell adhesion molecule, influences the aggressive nature of breast cancer cells, a potential connection to bone metastasis, Anticancer Res. 30 (2010) 1163–1168.
[8] S.R. Davies, C. Dent, G. Watkins, J.A. King, K. Mokbel, W.G. Jiang, Expression of the cell to cell adhesion molecule, ALCAM, in breast cancer patients and the potential link with skeletal metastasis, Oncol. Rep. 19 (2008) 555–561.
[9] M. Ihnen, N. Kohler, J.F. Kersten, K. Milde-Langosch, K. Beck, S. Holler, V. Muller, I. Witzel, F. Janicke, E. Kilic, Expression levels of Activated Leukocyte Cell Adhesion Molecule (ALCAM/CD166) in primary breast carcinoma and distant breast cancer metastases, Dis. Markers 28 (2010) 71–78.
[10] W. Weichert, T. Knosel, J. Bellach, M. Dietel, G. Kristiansen, ALCAM/CD166 is overexpressed in colorectal carcinoma and correlates with shortened patient survival, J. Clin. Pathol. 57 (2004) 1160–1164.
[11] M. Sawhney, A. Matta, M.A. Macha, J. Kaur, S. DattaGupta, N.K. Shukla, R. Ralhan, Cytoplasmic accumulation of activated leukocyte cell adhesion molecule is a predictor of disease progression and reduced survival in oral cancer patients, Int. J. Cancer 124 (2009) 2098–2105.
[12] M. van den Brand, R.P. Takes, M. Blokpoel-deRuyter, P.J. Slootweg, L.C. van Kempen, Activated leukocyte cell adhesion molecule expression predicts lymph node metastasis in oral squamous cell carcinoma, Oral Oncol. 46 (2010) 393–398.
[13] C. Kahlert, H. Weber, C. Mogler, F. Bergmann, P. Schirmacher, H.G. Kenngott, U. Matterne, N. Mollberg, N.N. Rahbari, U. Hinz, M. Koch, M. Aigner, J. Weitz, Increased expression of ALCAM/CD166 in pancreatic cancer is an independent prognostic marker for poor survival and early tumour relapse, Br. J. Cancer 101 (2009) 457–464.
[14] M.V. Corrias, C. Gambini, A. Gregorio, M. Croce, G. Barisione, C. Cossu, A. Rossello, S. Ferrini, M. Fabbi, Different subcellular localization of ALCAM molecules in neuroblastoma: association with relapse, Cell. Oncol. 32 (2010) 77–86.
[15] D. Mezzanzanica, M. Fabbi, M. Bagnoli, S. Staurengo, M. Losa, E. Balladore, P. Alberti, L. Lusa, A. Ditto, S. Ferrini, M.A. Pierotti, M. Barbareschi, S. Pilotti, S. Canevari, Subcellular localization of activated leukocyte cell adhesion molecule is a molecular predictor of survival in ovarian carcinoma patients, Clin. Cancer Res. 14 (2008) 1726–1733.
[16] L.C. van Kempen, J.J. van den Oord, G.N. van Muijen, U.H. Weidle, H.P. Bloemers, G.W. Swart, Activated leukocyte cell adhesion molecule/CD166, a marker of tumor progression in primary malignant melanoma of the skin, Am. J. Pathol. 156 (2000) 769–774.
[17] M. Burkhardt, E. Mayordomo, K.J. Winzer, F. Fritzsche, T. Gansukh, S. Pahl, W. Weichert, C. Denkert, H. Guski, M. Dietel, G. Kristiansen, Cytoplasmic overexpression of ALCAM is prognostic of disease progression in breast cancer, J. Clin. Pathol. 59 (2006) 403–409.
[18] G. Kristiansen, C. Pilarsky, C. Wissmann, C. Stephan, L. Weissbach, V. Loy, S. Loening, M. Dietel, A. Rosenthal, ALCAM/CD166 is up-regulated in low-grade prostate cancer and progressively lost in high-grade lesions, Prostate 54 (2003) 34–43.
[19] T. Piazza, E. Cha, I. Bongarzone, S. Canevari, A. Bolognesi, L. Polito, A. Bargellesi, F. Sassi, S. Ferrini, M. Fabbi, Internalization and recycling of ALCAM/CD166 detected by a fully human single-chain recombinant antibody, J. Cell Sci. 118 (2005) 1515–1525.
[20] K. Thelen, T. Georg, S. Bertuch, P. Zelina, G.E. Pollerberg, Ubiquitination and endocytosis of cell adhesion molecule DM-GRASP regulate its cell surface presence and affect its role for axon navigation, J. Biol. Chem. 283 (2008) 32792–32801.
[21] J.J. Bech-Serra, B. Santiago-Josefat, C. Esselens, P. Saftig, J. Baselga, J. Arribas, F. Canals, Proteomic identification of desmoglein 2 and activated leukocyte cell adhesion molecule as substrates of ADAM17 and ADAM10 by difference gel electrophoresis, Mol. Cell. Biol. 26 (2006) 5086–5095.
[22] O. Rosso, T. Piazza, I. Bongarzone, A. Rossello, D. Mezzanzanica, S. Canevari, A.M. Orengo, A. Puppo, S. Ferrini, M. Fabbi, The ALCAM shedding by the metalloprotease ADAM17/TACE is involved in motility of ovarian carcinoma cells, Mol. Cancer Res. 5 (2007) 1246–1253.
[23] V.M. Delgado, L.G. Nugnes, L.L. Colombo, M.F. Troncoso, M.M. Fernandez, E.L. Malchiodi, I. Frahm, D.O. Croci, D. Compagno, G.A. Rabinovich, C. Wolfenstein-Todel, M.T. Elola, Modulation of endothelial cell migration and angiogenesis: a novel function for the "tandem-repeat" lectin galectin-8, FASEB J. 25 (2011) 242–254.
[24] N. Bidon, F. Brichory, S. Hanash, P. Bourguet, L. Dazord, J.P. Le Pennec, Two messenger RNAs and five isoforms for Po66-CBP, a galectin-8 homolog in a human lung carcinoma cell line, Gene 274 (2001) 253–262.
[25] Y. Zick, M. Eisenstein, R.A. Goren, Y.R. Hadari, Y. Levy, D. Ronen, Role of galectin-8 as a modulator of cell adhesion and cell growth, Glycoconj. J. 19 (2004) 517–526.
[26] S. Carlsson, C.T. Oberg, M.C. Carlsson, A. Sundin, U.J. Nilsson, D. Smith, R.D. Cummings, J. Almkvist, A. Karlsson, H. Leffler, Affinity of galectin-8 and its carbohydrate recognition domains for ligands in solution and at the cell surface, Glycobiology 17 (2007) 663–676.
[27] H. Ideo, A. Seko, I. Ishizuka, K. Yamashita, The N-terminal carbohydrate recognition domain of galectin-8 recognizes specific glycosphingolipids with high affinity, Glycobiology 13 (2003) 713–723.
[28] Y.R. Hadari, R. Arbel-Goren, Y. Levy, A. Amsterdam, R. Alon, R. Zakut, Y. Zick, Galectin-8 binding to integrins inhibits cell adhesion and induces apoptosis, J. Cell Sci. 113 (2000) 2385–2397.
[29] Y. Levy, R. Arbel-Goren, Y.R. Hadari, S. Eshhar, D. Ronen, E. Elhanany, B. Geiger, Y. Zick, Galectin-8 functions as a matricellular modulator of cell adhesion, J. Biol. Chem. 276 (2001) 31285–31295.
[30] Y. Levy, D. Ronen, A.D. Bershadsky, Y. Zick, Sustained induction of ERK, protein kinase B, and p70 S6 kinase regulates cell spreading and formation of F-actin microspikes upon ligation of integrins by galectin-8, a mammalian lectin, J. Biol. Chem. 278 (2003) 14533–14542.
[31] N. Nishi, H. Shoji, M. Seki, A. Itoh, H. Miyanaka, K. Yuube, M. Hirashima, T. Nakamura, Galectin-8 modulates neutrophil function via interaction with integrin alphaM, Glycobiology 13 (2003) 755–763.
[32] L. Eshkar-Sebban, D. Ronen, D. Levartovsky, O. Elkayam, D. Caspi, S. Aamar, H. Amital, A. Rubinow, I. Golan, D. Naor, Y. Zick, I. Golan, The involvement of CD44 and its novel ligand galectin-8 in apoptotic regulation of autoimmune inflammation, J. Immunol. 179 (2007) 1225–1235.
[33] C. Zappelli, C. van der Zwaan, D.C. Thijssen-Timmer, K. Mertens, A.B. Meijer, Novel role for galectin-8 protein as mediator of coagulation factor V endocytosis by megakaryocytes, J. Biol. Chem. 287 (2012) 8327–8335.

Please cite this article as: M.M. Fernández, et al., Glycosylation-dependent binding of galectin-8 to activated leukocyte cell adhesion molecule (ALCAM/CD166) promotes its surface seg..., Biochim. Biophys. Acta (2016), http://dx.doi.org/10.1016/j.bbagen.2016.04.019

[34] L.N. Cueni, M. Detmar, Galectin-8 interacts with podoplanin and modulates lymphatic endothelial cell functions, Exp. Cell Res. 315 (2009) 1715–1723.
[35] T.L. Thurston, M.P. Wandel, N. von Muhlinen, A. Foeglein, F. Randow, Galectin 8 targets damaged vesicles for autophagy to defend cells against bacterial invasion, Nature 482 (2012) 414–418.
[36] R. Arbel-Goren, Y. Levy, D. Ronen, Y. Zick, Cyclin-dependent kinase inhibitors and JNK act as molecular switches, regulating the choice between growth arrest and apoptosis induced by galectin-8, J. Biol. Chem. 280 (2005) 19105–19114.
[37] S.R. Stowell, C.M. Arthur, M. Dias-Baruffi, L.C. Rodrigues, J.P. Gourdine, J. Heimburg-Molinaro, T. Ju, R.J. Molinaro, C. Rivera-Marrero, B. Xia, D.F. Smith, R.D. Cummings, Innate immune lectins kill bacteria expressing blood group antigen, Nat. Med. 16 (2010) 295–301.
[38] J.F. Sampson, A. Suryawanshi, W.S. Chen, G.A. Rabinovich, N. Panjwani, Galectin-8 promotes regulatory T-cell differentiation by modulating IL-2 and TGFbeta signaling, Immunol. Cell Biol. 94 (2016) 213–219.
[39] N. Bidon-Wagner, J.P. Le Pennec, Human galectin-8 isoforms and cancer, Glycoconj. J. 19 (2004) 557–563.
[40] A. Danguy, S. Rorive, C. Decaestecker, Y. Bronckart, H. Kaltner, Y.R. Hadari, R. Goren, Y. Zich, M. Petein, I. Salmon, H.J. Gabius, R. Kiss, Immunohistochemical profile of galectin-8 expression in benign and malignant tumors of epithelial, mesenchymatous and adipous origins, and of the nervous system, Histol. Histopathol. 16 (2001) 861–868.
[41] H. Lahm, S. Andre, A. Hoeflich, J.R. Fischer, B. Sordat, H. Kaltner, E. Wolf, H.J. Gabius, Comprehensive galectin fingerprinting in a panel of 61 human tumor cell lines by RT-PCR and its implications for diagnostic and therapeutic procedures, J. Cancer Res. Clin. Oncol. 127 (2001) 375–386.
[42] M.V. Espelt, D.O. Croci, M.L. Bacigalupo, P. Carabias, M. Manzi, M.T. Elola, M.C. Munoz, F.P. Dominici, C. Wolfenstein-Todel, G.A. Rabinovich, M.F. Troncoso, Novel roles of galectin-1 in hepatocellular carcinoma cell adhesion, polarization, and in vivo tumor growth, Hepatology 53 (2011) 2097–2106.
[43] M.M. Fernandez, S. Bhattacharya, M.C. De Marzi, P.H. Brown, M. Kerzic, P. Schuck, R.A. Mariuzza, E.L. Malchiodi, Superantigen natural affinity maturation revealed by the crystal structure of staphylococcal enterotoxin G and its binding to T-cell receptor Vbeta8.2, Proteins 68 (2007) 389–402.
[44] L. Royle, R.A. Dwek, P.M. Rudd, Determining the structure of oligosaccharides N- and O-linked to glycoproteins, Curr. Protoc. Protein Sci 2006, pp. 1–45.
[45] P.H. Jensen, N.G. Karlsson, D. Kolarich, N.H. Packer, Structural analysis of N- and O-glycans released from glycoproteins, Nat. Protoc. 7 (2012) 1299–1310.
[46] K. Mariño, J. Bones, J.J. Kattla, P.M. Rudd, A systematic approach to protein glycosylation analysis: a path through the maze, Nat. Chem. Biol. 6 (2010) 713–723.
[47] S. Diskin, Z. Cao, H. Leffler, N. Panjwani, The role of integrin glycosylation in galectin-8-mediated trabecular meshwork cell adhesion and spreading, Glycobiology 19 (2009) 29–37.
[48] H.R. Quinta, L.A. Pasquini, J.M. Pasquini, Three-dimensional reconstruction of corticospinal tract using one-photon confocal microscopy acquisition allows detection of axonal disruption in spinal cord injury, J. Neurochem. 133 (2015) 113–124.
[49] E.M.M. Manders, F.J. Verbeek, J.A. Aten, Measurement of co-localization of objects in dual-colour confocal images, J. Microsc. 169 (1993) 375–382.
[50] L.C. van Kempen, J.M. Nelissen, W.G. Degen, R. Torensma, U.H. Weidle, H.P. Bloemers, C.G. Figdor, G.W. Swart, Molecular basis for the homophilic activated leukocyte cell adhesion molecule (ALCAM)-ALCAM interaction, J. Biol. Chem. 276 (2001) 25783–25790.
[51] M.A. Bowen, A.A. Aruffo, J. Bajorath, Cell surface receptors and their ligands: in vitro analysis of CD6-CD166 interactions, Proteins 40 (2000) 420–428.
[52] N.J. Hassan, A.N. Barclay, M.H. Brown, Frontline: optimal T cell activation requires the engagement of CD6 and CD166, Eur. J. Immunol. 34 (2004) 930–940.
[53] J. Te Riet, A.W. Zimmerman, A. Cambi, B. Joosten, S. Speller, R. Torensma, F.N. van Leeuwen, C.G. Figdor, F. de Lange, Distinct kinetic and mechanical properties govern ALCAM-mediated interactions as shown by single-molecule force spectroscopy, J. Cell Sci. 120 (2007) 3965–3976.
[54] D.S. Kim, Y. Hahn, The acquisition of novel N-glycosylation sites in conserved proteins during human evolution, BMC Bioinformatics 16 (2015) 29.
[55] C. Raymond, A. Robotham, J. Kelly, E. Lattová, H. Perreault, Y. Durocher, Production of highly sialylated monoclonal antibodies, in: Stefana Petrescu (Ed.), Glycosylation, InTech 2012, p. 397.
[56] Y. Yuan, L. Wu, S. Shen, S. Wu, M.M. Burdick, Effect of alpha 2,6 sialylation on integrin-mediated adhesion of breast cancer cells to fibronectin and collagen IV, Life Sci. 149 (2016) 138–145.
[57] C. Escoda-Ferran, E. Carrasco, M. Caballero-Banos, C. Miro-Julia, M. Martinez-Florensa, M. Consuegra-Fernandez, V.G. Martinez, F.T. Liu, F. Lozano, Modulation of CD6 function through interaction with Galectin-1 and −3, FEBS Lett. 588 (2014) 2805–2813.
[58] G.A. Rabinovich, M.A. Toscano, Turning 'sweet' on immunity: galectin-glycan interactions in immune tolerance and inflammation, Nat. Rev. Immunol. 9 (2009) 338–352.
[59] C. Boscher, J.W. Dennis, I.R. Nabi, Glycosylation, galectins and cellular signaling, Curr. Opin. Cell Biol. 23 (2011) 383–392.
[60] J.W. Dennis, C.F. Brewer, Density-dependent lectin-glycan interactions as a paradigm for conditional regulation by posttranslational modifications, Mol. Cell. Proteomics 12 (2013) 913–920.
[61] M.T. Elola, A.G. Blidner, F. Ferragut, C. Bracalente, G.A. Rabinovich, Assembly, organization and regulation of cell-surface receptors by lectin-glycan complexes, Biochem. J. 469 (2015) 1–16.
[62] I.J. Chen, H.L. Chen, M. Demetriou, Lateral compartmentalization of T cell receptor versus CD45 by galectin-N-glycan binding and microfilaments coordinate basal and activation signaling, J. Biol. Chem. 282 (2007) 35361–35372.
[63] S.C. Starossom, I.D. Mascanfroni, J. Imitola, L. Cao, K. Raddassi, S.F. Hernandez, R. Bassil, D.O. Croci, J.P. Cerliani, D. Delacour, Y. Wang, W. Elyaman, S.J. Khoury, G.A. Rabinovich, Galectin-1 deactivates classically activated microglia and protects from inflammation-induced neurodegeneration, Immunity 37 (2012) 249–263.
[64] D.O. Croci, J.P. Cerliani, T. Dalotto-Moreno, S.P. Mendez-Huergo, I.D. Mascanfroni, S. Dergan-Dylon, M.A. Toscano, J.J. Caramelo, J.J. Garcia-Vallejo, J. Ouyang, E.A. Mesri, M.R. Junttila, C. Bais, M.A. Shipp, M. Salatino, G.A. Rabinovich, Glycosylation-dependent lectin-receptor interactions preserve angiogenesis in anti-VEGF refractory tumors, Cell 156 (2014) 744–758.
[65] C. Boscher, Y.Z. Zheng, R. Lakshminarayan, L. Johannes, J.W. Dennis, L.J. Foster, I.R. Nabi, Galectin-3 protein regulates mobility of N-cadherin and GM1 ganglioside at cell-cell junctions of mammary carcinoma cells, J. Biol. Chem. 287 (2012) 32940–32952.
[66] K.S. Lau, E.A. Partridge, A. Grigorian, C.I. Silvescu, V.N. Reinhold, M. Demetriou, J.W. Dennis, Complex N-glycan number and degree of branching cooperate to regulate cell proliferation and differentiation, Cell 129 (2007) 123–134.
[67] E.A. Partridge, C. Le Roy, G.M. Di Guglielmo, J. Pawling, P. Cheung, M. Granovsky, I.R. Nabi, J.L. Wrana, J.W. Dennis, Regulation of cytokine receptors by Golgi N-glycan processing and endocytosis, Science 306 (2004) 120–124.
[68] G. Carbotti, A.M. Orengo, D. Mezzanzanica, M. Bagnoli, A. Brizzolara, L. Emionite, A. Puppo, M.G. Centurioni, M. Bruzzone, P. Marroni, A. Rossello, S. Canevari, S. Ferrini, M. Fabbi, Activated leukocyte cell adhesion molecule soluble form: a potential biomarker of epithelial ovarian cancer is increased in type II tumors, Int. J. Cancer 132 (2013) 2597–2605.
[69] D. Piao, T. Jiang, G. Liu, B. Wang, J. Xu, A. Zhu, Clinical implications of activated leukocyte cell adhesion molecule expression in breast cancer, Mol. Biol. Rep. 39 (2012) 661–668.
[70] E. Burandt, T. Bari Noubar, A. Lebeau, S. Minner, C. Burdelski, F. Janicke, V. Muller, L. Terracciano, R. Simon, G. Sauter, W. Wilczak, P. Lebok, Loss of ALCAM expression is linked to adverse phenotype and poor prognosis in breast cancer: a TMA-based immunohistochemical study on 2,197 breast cancer patients, Oncol. Rep. 32 (2014) 2628–2634.
[71] F. Tan, M. Mosunjac, A.L. Adams, B. Adade, O. Taye, Y. Hu, M. Rizzo, S.F. Ofori-Acquah, Enhanced down-regulation of ALCAM/CD166 in African-American Breast Cancer, BMC Cancer 14 (2014) 715.
[72] H. Lu, K.L. Knutson, E. Gad, M.L. Disis, The tumor antigen repertoire identified in tumor-bearing neu transgenic mice predicts human tumor antigens, Cancer Res. 66 (2006) 9754–9761.
[73] H.E. Miwa, W.R. Koba, E.J. Fine, O. Giricz, P.A. Kenny, P. Stanley, Bisected, complex N-glycans and galectins in mouse mammary tumor progression and human breast cancer, Glycobiology 23 (2013) 1477–1490.
[74] Y. Vinik, H. Shatz-Azoulay, A. Vivanti, N. Hever, Y. Levy, R. Karmona, V. Brumfeld, S. Baraghithy, M. Attar-Lamdar, S. Boura-Halfon, I. Bab, Y. Zick, The mammalian lectin galectin-8 induces RANKL expression, osteoclastogenesis, and bone mass reduction in mice, Elife 4 (2015), e05914.
[75] J.F. Sampson, A. Suryawanshi, W.S. Chen, G.A. Rabinovich, N. Panjwani, Galectin-8 promotes regulatory T-cell differentiation by modulating IL-2 and TGFbeta signaling, Immunol. Cell Biol. 94 (2016) 213–219.
[76] K. Fujiwara, K. Ohuchida, M. Sada, K. Horioka, C.D. Ulrich III, K. Shindo, T. Ohtsuka, S. Takahata, K. Mizumoto, Y. Oda, M. Tanaka, CD166/ALCAM expression is characteristic of tumorigenicity and invasive and migratory activities of pancreatic cancer cells, PLoS One 9 (2014) e107247.
[77] M.L. Bacigalupo, M. Manzi, M.V. Espelt, L.D. Gentilini, D. Compagno, D.J. Laderach, C. Wolfenstein-Todel, G.A. Rabinovich, M.F. Troncoso, Galectin-1 triggers epithelial-mesenchymal transition in human hepatocellular carcinoma cells, J. Cell. Physiol. 230 (2015) 1298–1309.
[78] A. Santiago-Gomez, J.I. Barrasa, N. Olmo, E. Lecona, H. Burghardt, M. Palacin, M.A. Lizarbe, J. Turnay, 4F2hc-silencing impairs tumorigenicity of HeLa cells via modulation of galectin-3 and beta-catenin signaling, and MMP-2 expression, Biochim. Biophys. Acta 1833 (2013) 2045–2056.
[79] L.P. Wang, S.W. Chen, S.M. Zhuang, H. Li, M. Song, Galectin-3 accelerates the progression of oral tongue squamous cell carcinoma via a Wnt/beta-catenin-dependent pathway, Pathol. Oncol. Res. 19 (2013) 461–474.
[80] S.E. Singletary, C. Allred, P. Ashley, L.W. Bassett, D. Berry, K.I. Bland, P.I. Borgen, G.M. Clark, S.B. Edge, D.F. Hayes, L.L. Hughes, R.V. Hutter, M. Morrow, D.L. Page, A. Recht, R.L. Theriault, A. Thor, D.L. Weaver, H.S. Wieand, F.L. Greene, Staging system for breast cancer: revisions for the 6th edition of the AJCC Cancer Staging Manual, Surg. Clin. North Am. 83 (2003) 803–819.
[81] A.C. Wolff, M.E. Hammond, D.G. Hicks, M. Dowsett, L.M. McShane, K.H. Allison, D.C. Allred, J.M. Bartlett, M. Bilous, P. Fitzgibbons, W. Hanna, R.B. Jenkins, P.B. Mangu, S. Paik, E.A. Perez, M.F. Press, P.A. Spears, G.H. Vance, G. Viale, D.F. Hayes, Recommendations for human epidermal growth factor receptor 2 testing in breast cancer: American Society of Clinical Oncology/College of American Pathologists clinical practice guideline update, J. Clin. Oncol. 31 (2013) 3997–4013.

Please cite this article as: M.M. Fernández, et al., Glycosylation-dependent binding of galectin-8 to activated leukocyte cell adhesion molecule (ALCAM/CD166) promotes its surface seg..., Biochim. Biophys. Acta (2016), http://dx.doi.org/10.1016/j.bbagen.2016.04.019